2021-06

DESIGN AND ANALYSIS OF A MACH 5+ HYPERSONIC WIND TUNNEL

Aspray, Connor J.

Monterey, CA; Naval Postgraduate School

NAVAL POSTGRADUATE SCHOOL

MONTEREY, CALIFORNIA

THESIS

DESIGN AND ANALYSIS OF A MACH 5+ HYPERSONIC WIND TUNNEL

by

Connor J. Aspray

June 2021

Thesis Advisor:	Garth V. Hobson
Co-Advisor:	Anthony J. Gannon
Second Reader:	Walter Smith

THIS PAGE INTENTIONALLY LEFT BLANK

REPORT DOCUMENTATION PAGE			*Form Approved OMB No. 0704-0188*

1. AGENCY USE ONLY *(Leave blank)*	**2. REPORT DATE** June 2021	**3. REPORT TYPE AND DATES COVERED** Master's thesis

4. TITLE AND SUBTITLE
DESIGN AND ANALYSIS OF A MACH 5+ HYPERSONIC WIND TUNNEL

5. FUNDING NUMBERS

6. AUTHOR(S) Connor J. Aspray

7. PERFORMING ORGANIZATION NAME(S) AND ADDRESS(ES)
Naval Postgraduate School
Monterey, CA 93943-5000

8. PERFORMING ORGANIZATION REPORT NUMBER

9. SPONSORING / MONITORING AGENCY NAME(S) AND ADDRESS(ES)
N/A

10. SPONSORING / MONITORING AGENCY REPORT NUMBER

11. SUPPLEMENTARY NOTES The views expressed in this thesis are those of the author and do not reflect the official policy or position of the Department of Defense or the U.S. Government.

12a. DISTRIBUTION / AVAILABILITY STATEMENT
Approved for public release. Distribution is unlimited.

12b. DISTRIBUTION CODE
A

13. ABSTRACT (maximum 200 words)

Hypersonics sits atop a short list of Department of Defense research priorities outlined by the 2018 National Defense Strategy. The Naval Postgraduate School is uniquely equipped to contribute to this research as the current configuration of the gas dynamics laboratory is capable, with modifications, of facilitating long-runtime, high-Mach number flows. These long runtime flows will be capable of providing data for experiments in hypersonic shock-boundary layer interaction and ram/scramjet inlet design and analysis. Accordingly, this paper develops a design modification to upgrade the current Mach 4 wind tunnel into one capable of producing uniform Mach numbers greater than 5.0 for runtimes longer than 20 minutes. In the process, a method of computational fluid dynamics was developed to assess, modify, and redesign nozzles produced by an inviscid method of characteristics design tool to account for viscous effects. The computationally designed curves were then utilized to design hardware to be later procured to build and operate the tunnel. In addition to a modified tunnel geometry, an additional heater is required to ensure that the flow does not liquefy during expansion. The size and power of this heater to achieve Mach 5.0 flows was calculated. Finally, this project provides a foundation for later work in hardware procurement and tunnel construction to make NPS one of a handful of institutions capable of conduction research in hypersonics in the United States.

14. SUBJECT TERMS
hypersonics, wind tunnels, compressible flows, computational fluid dynamics, design, supersonic wind tunnel, hypersonic wind tunnel, corner vortices

15. NUMBER OF PAGES
63

16. PRICE CODE

17. SECURITY CLASSIFICATION OF REPORT	**18. SECURITY CLASSIFICATION OF THIS PAGE**	**19. SECURITY CLASSIFICATION OF ABSTRACT**	**20. LIMITATION OF ABSTRACT**
Unclassified	Unclassified	Unclassified	UU

NSN 7540-01-280-5500

Standard Form 298 (Rev. 2-89)
Prescribed by ANSI Std. 239-18

THIS PAGE INTENTIONALLY LEFT BLANK

Approved for public release. Distribution is unlimited.

DESIGN AND ANALYSIS OF A MACH 5+ HYPERSONIC WIND TUNNEL

Connor J. Aspray
Ensign, United States Navy
BS, United States Naval Academy, 2020

Submitted in partial fulfillment of the
requirements for the degree of

**MASTER OF SCIENCE IN ENGINEERING SCIENCE
(AEROSPACE ENGINEERING)**

from the

**NAVAL POSTGRADUATE SCHOOL
June 2021**

Approved by: Garth V. Hobson
Advisor

Anthony J. Gannon
Co-Advisor

Walter Smith
Second Reader

Garth V. Hobson
Chair, Department of Mechanical and Aerospace Engineering

THIS PAGE INTENTIONALLY LEFT BLANK

ABSTRACT

Hypersonics sits atop a short list of Department of Defense research priorities outlined by the 2018 National Defense Strategy. The Naval Postgraduate School is uniquely equipped to contribute to this research as the current configuration of the gas dynamics laboratory is capable, with modifications, of facilitating long-runtime, high-Mach number flows. These long runtime flows will be capable of providing data for experiments in hypersonic shock-boundary layer interaction and ram/scramjet inlet design and analysis. Accordingly, this paper develops a design modification to upgrade the current Mach 4 wind tunnel into one capable of producing uniform Mach numbers greater than 5.0 for runtimes longer than 20 minutes. In the process, a method of computational fluid dynamics was developed to assess, modify, and redesign nozzles produced by an inviscid method of characteristics design tool to account for viscous effects. The computationally designed curves were then utilized to design hardware to be later procured to build and operate the tunnel. In addition to a modified tunnel geometry, an additional heater is required to ensure that the flow does not liquefy during expansion. The size and power of this heater to achieve Mach 5.0 flows was calculated. Finally, this project provides a foundation for later work in hardware procurement and tunnel construction to make NPS one of a handful of institutions capable of conduction research in hypersonics in the United States.

THIS PAGE INTENTIONALLY LEFT BLANK

TABLE OF CONTENTS

THIS PAGE INTENTIONALLY LEFT BLANK

LIST OF FIGURES

LIST OF TABLES

THIS PAGE INTENTIONALLY LEFT BLANK

ACKNOWLEDGMENTS

I would like to thank Professors Garth Hobson, Anthony Gannon, and Walter Smith for their time and assistance in pursuit of this project. All the hours spent in the turbo lab allow me to walk away knowing a great deal more than when I arrived.

I am thankful to my undergraduate professors, specifically CAPT Scott Drayton, Maj Thompson Graves, Professor Gabriel Karpouzian, Professor David Miklosovic, CAPT Rob Niewoehner, and Maj Ben Switzer, for equipping me with the tools to pursue higher education.

I would also like to thank my family, specifically my parents, Richard and Susan Aspray, for their unwavering support throughout my life to enable me to study for and receive this degree and do everything else. I am forever indebted to you.

THIS PAGE INTENTIONALLY LEFT BLANK

I. INTRODUCTION

Hypersonic weapons development falls atop a short list of Department of Defense (DOD) research priorities outlined by the 2018 National Defense Strategy [1]. Vehicles capable of flight in the hypersonic regime are also mentioned in this document as one of the very technologies that will enable the United States to fight and win the wars of the future. As these new technologies are expanded to a greater number of countries with lower barriers of entry, it is imperative that the U.S. rapidly invest in systems that will provide the means for groundbreaking research in academic and defense contexts.

A 2004 study conducted by the RAND Corporation assessed the United States' wind tunnel and propulsion test facilities and the ability of the National Aeronautics and Space Administration (NASA) to serve national needs [2]. In the study, 10 tunnels were revealed to have the ability to support research at Mach numbers greater than 5.0. A summary table of these facilities and their capabilities is shown in Table 1.

Table 1 Active U.S. hypersonic wind tunnels from 2004 RAND report. Adapted from [2].

FACILITY	MACH #	RUN TIME (S)	TEST AREA (M^2)
NASA GLENN	5,6,7	103, 42, 90	0.8935
NASA LANGLEY 8HTT	3, 4, 5, 6.5		4.667124
NASA LANGLEY ARC-HEATED SCRAMJET TEST FACILITY	4.7, 6.0	120	0.08000, 0.07610
AFRL MACH 6 HIGH RN	6	240	0.07290
AFRL 20 INCH HYPERSONIC TUNNEL	12, 14		0.2026
AF VKF TUNNEL A	5.5	continuous	
AF VKF TUNNEL B	6, 8	continuous	1.266
AF VKF TUNNEL C	4,8,10	continuous	
AF VKF TUNNEL D	5	300	0.09290
HYPERVELOCITY WIND TUNNEL 9	7, 9, 10, 14	15	1.824

Though several tunnels are likely to have come online since the research was conducted for this report, several of the tunnels listed are likely inactive today. Therefore, the addition of a Mach 5+ wind tunnel at the Naval Postgraduate School (NPS) has the potential to greatly enhance the research capabilities of government agencies, academic institutions, and industry partners alike. NPS is also uniquely situated to provide such an enhancement when the current configuration of its gas dynamics laboratory is considered. The air supply system already in place, especially the volume of compressed air and the duct work, enable the transition from the Mach 4.0 to the Mach 5+ tunnel to take place under a realistic budget when compared with the construction of a new facility.

The combination of the national imperative and the capabilities already in place provide the groundwork for a project that NPS can reasonably and should definitely complete. Not only would it enable NPS faculty and students to study and advance the cutting edge of high Mach number flight vehicles, but a Mach 5+ tunnel would also allow NPS to uphold its mission of "advancing the operational effectiveness, technological leadership, and warfighting advantage of the Naval service" [3].

II. DESIGN REQUIREMENTS

Though the principles of generating a high Mach number flow field like the one currently present in the Mach 4 wind tunnel are identical in the case of a Mach 5+ tunnel, special considerations must be made with increasing Mach number. Not only will the interior geometry of the tunnel need to be modified to produce the flow field, but the range of temperatures and pressures within the tunnel will span beyond the range at which oxygen and nitrogen remain gaseous. Therefore, increasing the enthalpy of the flow field will be imperative to ensuring the principles of dynamic similarity are met in the tunnel. These and other high-level considerations of the tunnel's design and construction will be discussed in this chapter.

A. METRICS OF TUNNEL CAPABILITY

Similar to those listed in Table 2, tunnel capability is defined by such things as run time and test section size. Also useful for design purposes are the pressures, temperatures, and mass flow rates in the test section. This will give an idea as to the usefulness of any results obtained from the flow field in question. It is important to acknowledge that these calculations assumed ideal gas behavior and that the fluid may condense under real conditions. This issue will be further discussed later.

Table 2 Value summary for current and modified wind tunnel.

TEST SECTION MACH #	4.0	5.2
TEST SECTION AREA	0.01032 m^2 (16.0 in^2)	0.01032 m^2 (16.0 in^2)
STATIC PRESSURE	4.87 kPa	1.09 kPa
STATIC TEMPERATURE	68.5 K	76.1 K
STATIC DENSITY	0.248 kg/m^3	0.0501 kg/m^3
VELOCITY	664 m/s	909 m/s
REYNOLD'S NUMBER	918000	427000
RUN TIME	26 min	55 min
SIMULATED ALTITUDE	8230 m	16000 m
MASS FLOW RATE	1.67 kg/s	0.471 kg/s

When the run times in Table 2 are compared with those of Table 1, it becomes clear that NPS is uniquely equipped to offer an extremely high-runtime tunnel. High-runtime is a highly advantageous characteristic that will allow researchers to perform experiments requiring a large array of data during a single run of the wind tunnel. The types of experiments that will benefit from these runtimes are alpha sweeps, boundary layer surveys, and those experiments involving air-breathing propulsion and inlet design. Typically, researchers have only a few seconds or minutes at their disposal to stabilize the tunnel and collect the data they need before waiting hours for their compressed air storage to recharge.

The metrics most valued in a wind tunnel of this caliber are test section size, run time, and test section Mach number. Therefore, the tunnel was designed to accommodate each parameter and provide the most cost-effective solution to conduct high-speed fluids experiments.

B. SIZE REQUIREMENTS

Given the space in which the tunnel is being constructed, adherence to a set maximum measurement is required. However, size is also a factor in the runtime calculations as well as in the experimental capabilities of the wind tunnel. For reasons that will be discussed in Chapter III, it was decided to implement a rectangular cross sectional area tunnel with an asymmetric nozzle geometry. This means as the test section grows larger, the length of the overall tunnel will grow significantly, as will the thickness of the boundary layers produced by a high Mach number flow field.

Though a larger test section would enable experiments utilizing larger scale models and a wider range of test articles, it would reduce the run time of the wind tunnel and increase the manufacturing cost substantially. Because the goal of the NPS Mach 5+ tunnel is to offer high-runtime capabilities, the need to balance sufficient test article size while maintaining a flow field for 20+ minutes was an important design specification. This concept will be demonstrated in the next several equations. In equation (1),

$$A^* = MA\left(\frac{1+\left(\frac{\gamma-1}{2}\right)M^2}{\frac{\gamma+1}{2}}\right)^{-\left(\frac{\gamma+1}{2(\gamma-1)}\right)} \tag{1}$$

A^* is the throat area, A is the test section area, γ is the ratio of specific heats, and M is the test section Mach number. This relation describes the throat area as it relates to the test section area and Mach number. Equation (2) shows the relation necessary for design and runtime calculations for a nozzle with a second throat

$$P_t = \left(\frac{\left(\frac{\gamma+1}{2}\right)M_2^2}{1+\left(\frac{\gamma-1}{2}\right)M_2^2}\right)^{-\frac{\gamma}{\gamma-1}} \left(\frac{2\gamma}{\gamma+1}M_2^2 - \frac{\gamma-1}{\gamma+1}\right)^{-\frac{1}{1-\gamma}} P_a \ , \tag{2}$$

where P_a is atmospheric pressure, P_t is the stagnation temperature, and M_2 is the Mach number preceding the terminating normal shock (dependent on the second throat area). This ratio is key to the calculation of the mass flow, and thus the runtime, because the stagnation pressure (P_t) required to maintain the flow field will be the limiting factor on the mass of air available for a tunnel run of any duration. In Equation (3)

$$\dot{m} = \frac{A^* P_t}{\sqrt{RT_t}}\sqrt{\gamma}\left(\frac{2}{\gamma+1}\right)^{\frac{\gamma+1}{2(\gamma-1)}} \tag{3}$$

$\dot{m}$ is the mass flow rate, T_t is the stagnation temperature, and R is the ideal gas constant. This equation makes clear that mass flow rate, and thus tunnel runtime, are directly proportional to the nozzle throat area and the stagnation pressure. Equation (4) is used to calculate the tunnel runtime.

$$t = \frac{\left(P_i - P_f\right)\frac{MV}{RT}}{\dot{m}} \tag{4}$$

P_i is the initial tank pressure, P_f is the final tank pressure (equal to P_t), M is the molecular weight of the gas, V is the total volume of air, and T is the temperature of the gas in the

tank. Mass flow rate aside, this equation points to the fact that the higher the final pressure ($P_f = P_t$), the smaller the difference from the initial pressure and thus the lower the runtime. However, the effect of an increasing test section area and Mach number is compounded by the fact that those variables also increase the mass flow rate, thus shortening the runtime even further. Therefore, every millimeter by which the test section grows will decrease the runtime exponentially. Considering this, it was decided that the current 101.6-mm-by-101.6-mm test section configuration accommodated all the necessary geometries and experimental equipment; therefore, it was retained to allow maximization of the runtime in every scenario.

C. HEATING REQUIREMENTS

Another important consideration in tunnel design is the static pressures and temperatures inside the test section. In low Mach number supersonic tunnels, this is not typically a concern because the ambient temperatures and pressures inside the test section do not risk condensation and solidification of the gaseous species making up the air being forced through the nozzle. In the region of Mach 5+, however, these temperatures and pressures become more concerning [4] if expanding from atmospheric temperatures.

Isentropic flow relationships dictate that at a given Mach number, the static temperature of a fluid will be a certain fraction of its total temperature. In the case of the planned wind tunnel, at Mach 5.0, this static to total pressure ratio is approximately 16.7% of the total temperature [4]. When considering the fact that, unheated, the total temperature is only 288K, the static temperature in the tunnel falls somewhere around 48K. Even at the low ambient pressure inside the test section, this is a cryogenically low temperature. The implication of these conditions is that the gaseous species making up the air, namely nitrogen and oxygen, begin to condense and solidify at temperatures greater than that. Liquid oxygen has a freezing point of 56K and a boiling point of 90K at atmospheric pressure. Liquid nitrogen has freezing and boiling points of 63K and 77K respectively at atmospheric pressure. At the lower static pressures in the test section, nitrogen and oxygen have boiling points of 63K and 61K respectively [5]. Therefore, without increasing the enthalpy of the flow, one risks sending liquid and solid nitrogen and oxygen at whatever

potentially sensitive and expensive equipment is being used to gather experimental data. Damage to equipment aside, even if the test articles were robust enough, the specific heat ratios of the fluid at these low temperatures will no longer be 1.4 (approximately 1.56) [5], thus losing the implications of dynamic similarity.

Consulting the isobaric properties of nitrogen and oxygen at low temperatures, it was decided that a comfortable ambient temperature to avoid these saturation issues is approximately 80K. However, increasing the static temperature of the flow to this temperature is not as simple as increasing the inlet temperature by 30K. Instead, the inlet stagnation temperature must be raised by 180K to avoid the condensation risk in the test section. To be especially safe, however, it was decided that a temperature increase of 200K would be necessary to ensure that the ratio of specific heats of the gas was maintained at 1.4.

D. ADDITIONAL REQUIREMENTS

There are several other incorporations to keep in mind throughout the design process of the tunnel. Foremost among them are the integration of support equipment. Though the tunnel should have no issue fitting seamlessly into the current air supply system given the ducting already in place, the ease of operation is another consideration. The desire for the tunnel to be operable by a singular lab technician is also a design consideration [4]. This means that one person ought to be able to control the air supply system, the pressure valve and regulator, the heat exchanger, and any experimental equipment simultaneously. Ensuring this requirement is met will necessitate conscious decisions on the type of hardware purchased and installed throughout the system required to operate the tunnel.

Also key to the tunnel's usefulness will be the incorporation of experimentation. Schlieren/shadowgraph as well as particle image velocimetry will have space requirements to minimize distortion and maximize data quality and quantity. The tunnel design should be able to accommodate various measurement devices to include pitot-static probes, a sting balance, and any windows for the imaging methods. Finally, supporting stands to hold the weight of the components are not trivial. The test section itself is likely to weigh hundreds

of kilograms. Minimizing displacement of the air supply and the individual supporting components is key to a tunnel that is well designed and feasible for decades of use.

III. NOZZLE DESIGN PROCESS

This chapter serves to detail the process by which the nozzle was designed and validated to produce the desired test section Mach number and flow qualities. This is central to the design process as each Mach number requires a unique nozzle to expand the flow uniformly and with the greatest efficiency. Initially, a MATLAB code was used to design a nozzle geometry according to the inviscid method of characteristics (Dodson [6]). Then, extensive work was performed in ANSYS CFX computational fluid dynamics software to ensure the design met all thresholds before any money is spend on producing a physical model.

A. VALIDATION OF CFD METHOD

After utilizing engineering drawings to replicate the current Mach 4 geometry, the effectiveness of the nozzle's design was assessed. Because of the cost and facilities required to test such geometries in an experimental setting, ANSYS CFX was utilized to provide a simulation of the effect of the expected conditions on the actual flow field generated.

First and foremost to this task was developing a robust CFD method by which each geometry could be tested. At first glance, a compressible fluid simulation through a converging-diverging nozzle should be relatively straightforward. However, for those who are unfamiliar, CFD, especially in the case of highly compressible, dual-throated flows like those discussed here, can be particularly idiosyncratic. Because of the inclusion of the second throat in the nozzle geometry and the supersonic outlet boundary condition, the flow field had to be developed gradually and in a manner closely modeling the real physics of the tunnel starting. This process took weeks, involving numerous changes in geometry, boundary conditions, mesh refinements, and software. A full summary of this process is explained in several pages of detail in the report titled "Employing the Method of Characteristics in Supersonic Nozzle Design" included in Appendix A. To summarize it briefly, the inlet stagnation pressure was gradually increased in a course mesh to produce a supersonic flow before the first nozzle throat, and then the outlet boundary condition was

changed to fully form the supersonic flow field. Once a stable solution was achieved in a course mesh, the mesh was refined to reveal greater physical accuracy in the results.

To mitigate the development of a method yielding physically inaccurate results, the current Mach 4.0 geometry was utilized. The developed method would need to achieve experimentally verifiable results prior to being tests on new geometries.

Initial results in the Mach 4 test case looked promising. Inviscid simulations revealed a test section Mach number just above the design of 4.0. The mesh utilized consisted of 267,000 nodes and 176,000 elements and is shown in Figure 1 and Figure 2. The symmetry plane and test section Mach number distributions are shown in Figure 3 and Figure 4. The plot of the root-mean-squared residuals is included in Appendix B.

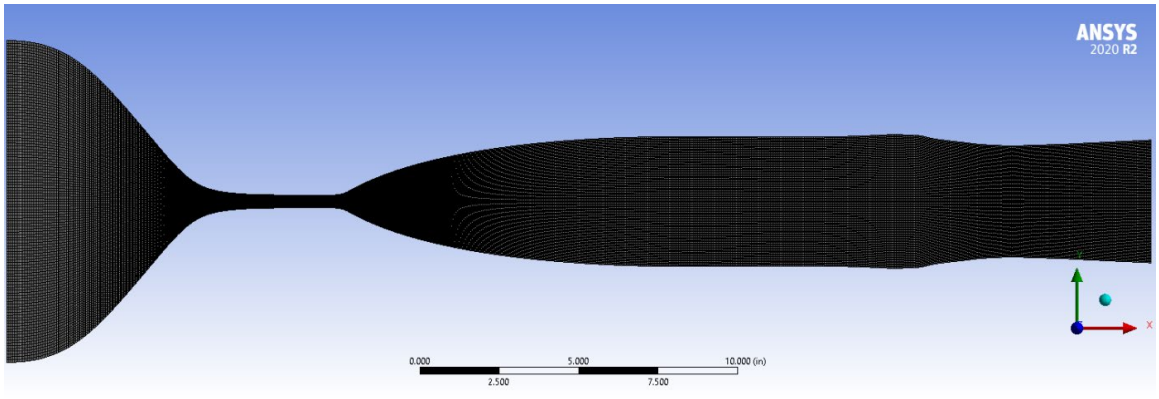

Figure 1 Mesh utilized in 2D, inviscid Mach 4 nozzle simulation.

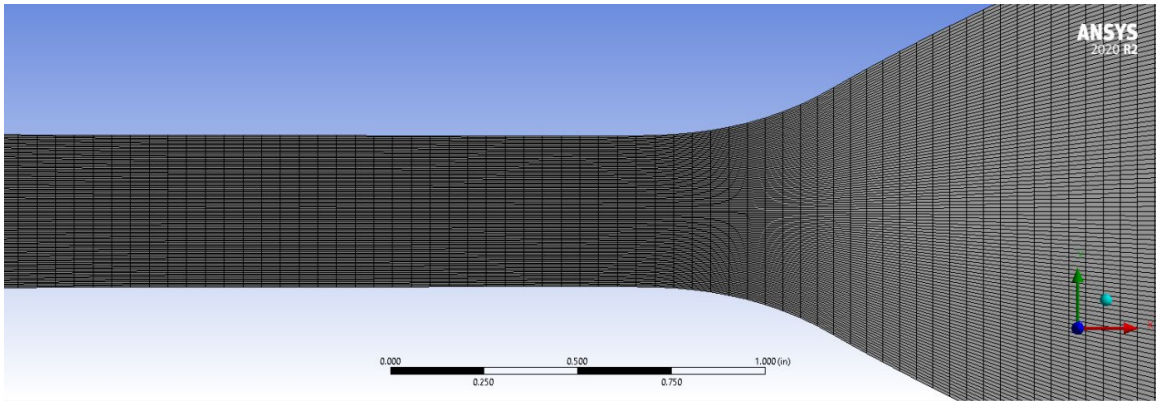

Figure 2 Zoomed in view of throat exit mesh corresponding to Figure 1.

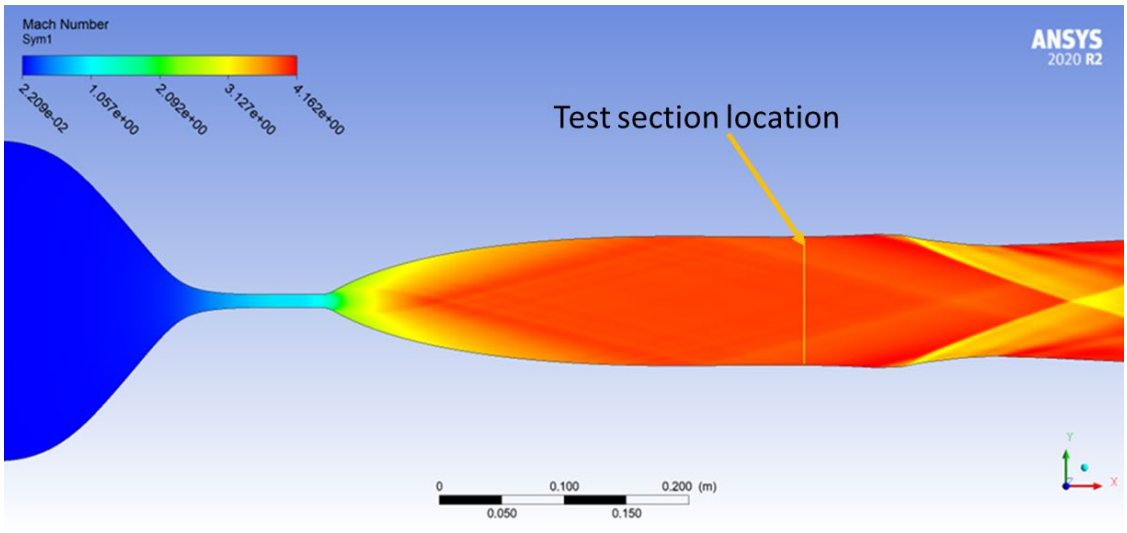

Figure 3 Inviscid solution Mach number distribution in XY plane of Mach 4 nozzle.

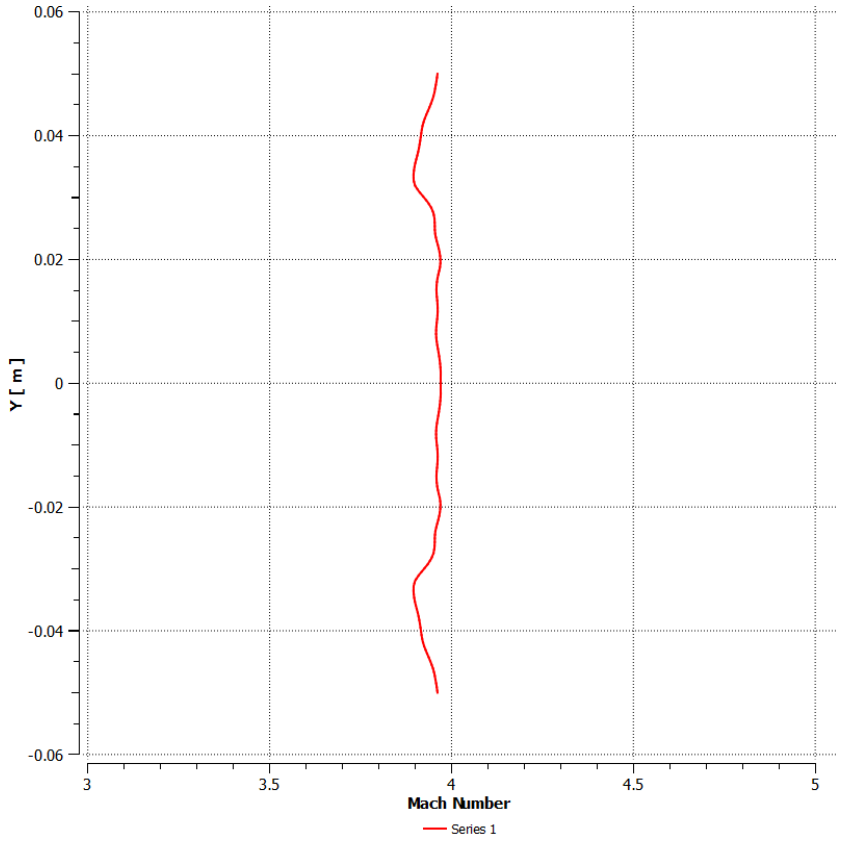

Figure 4 Inviscid solution test section Mach number distribution in Mach 4 nozzle.

Figure 3 shows the Mach number distribution along the symmetry plane of the entire nozzle. The flow gradually accelerates to Mach 1 through the nozzle throat and expands to approximately Mach 3.95 in the diverging section of the nozzle. Note the small range of Mach numbers and lack of boundary layers along the Y-axis in the test section of the nozzle. Achieving a Mach number so close to that of the design in CFD was certainly encouraging. However, this solution was not comparable to any of the experimental data considering that it ignores viscous forces of the fluid and the change in effective area brought about by the boundary layer growth. So, a viscous, fully turbulent shear stress transport model was implemented to resolve the boundary layers and better understand the real flow field. These results are depicted visually in Figure 5 and Figure 6.

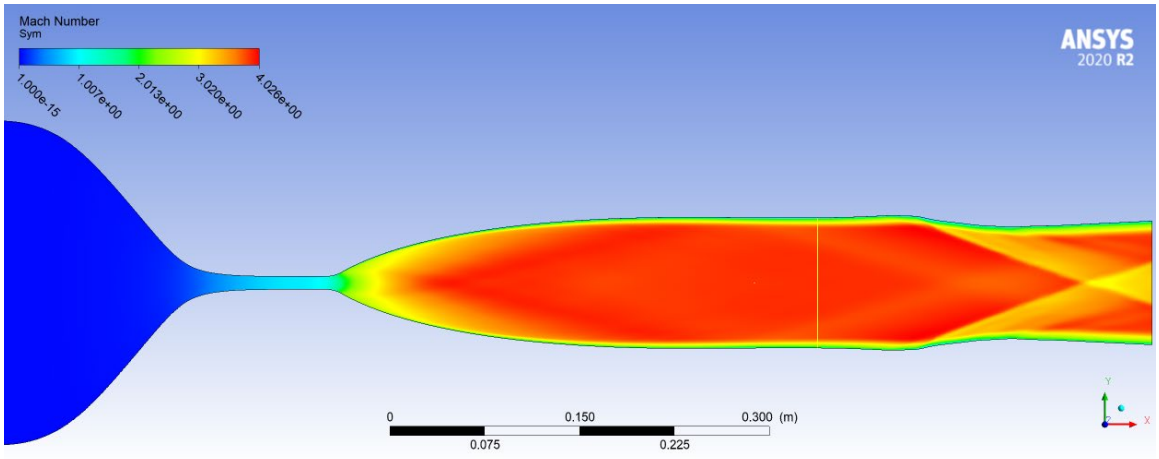

Figure 5 Viscous, turbulent solution with shear stress transport turbulence model, Mach 4 nozzle.

The fully viscous simulation imbued confidence in the method by returning results closely matching the target Mach number and boundary layer thickness. This method was then applied to the same Mach 4 nozzle with a diamond shaped airfoil in the test section. The purpose of this test case was to compare the calculated data with the experimental data to ensure the proper test conditions were being set and achieved in the CFX software. The static pressure on each face of the diamond-shaped airfoil was calculated from the CFD simulation and compared to data gathered experimentally in the Mach 4 wind tunnel. The CFD results can be observed in Figure 7 and Figure 8.

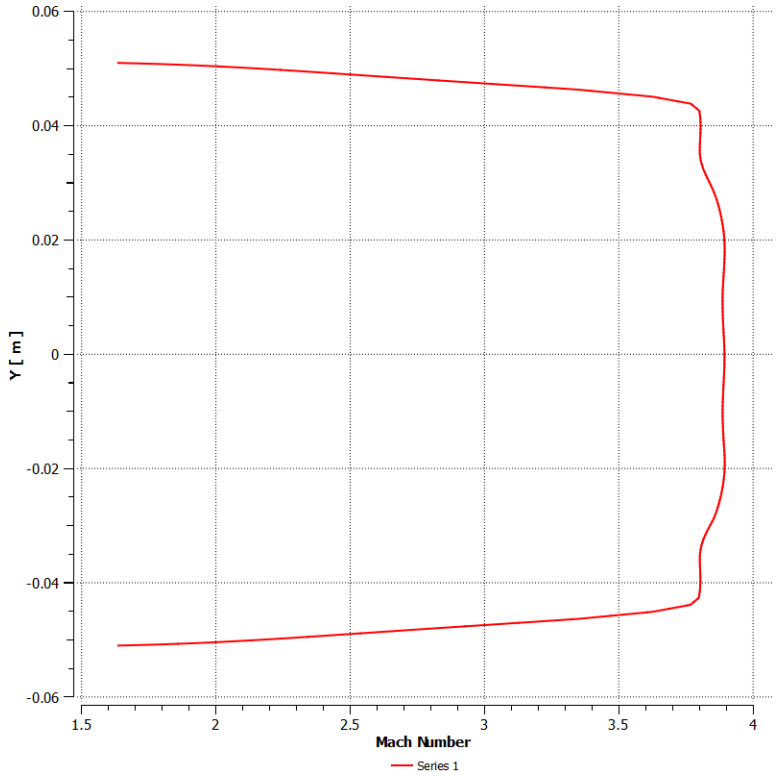

Figure 6 Viscous, turbulent solution test section Mach number distribution, Mach 4 nozzle.

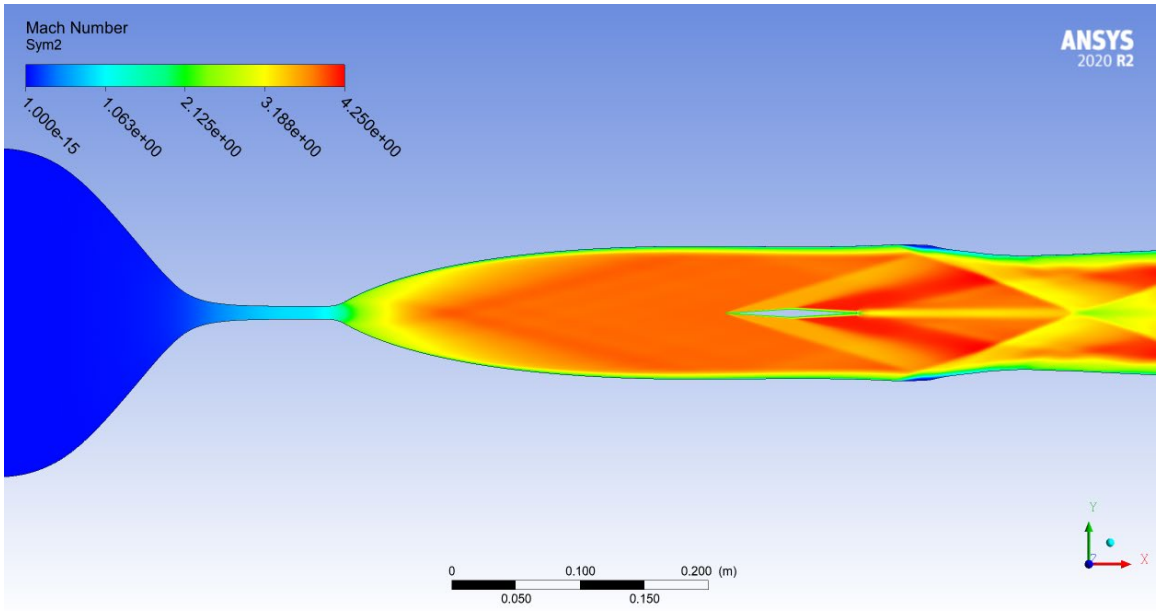

Figure 7 Viscous, turbulent Mach 4 solution with diamond shaped airfoil solution.

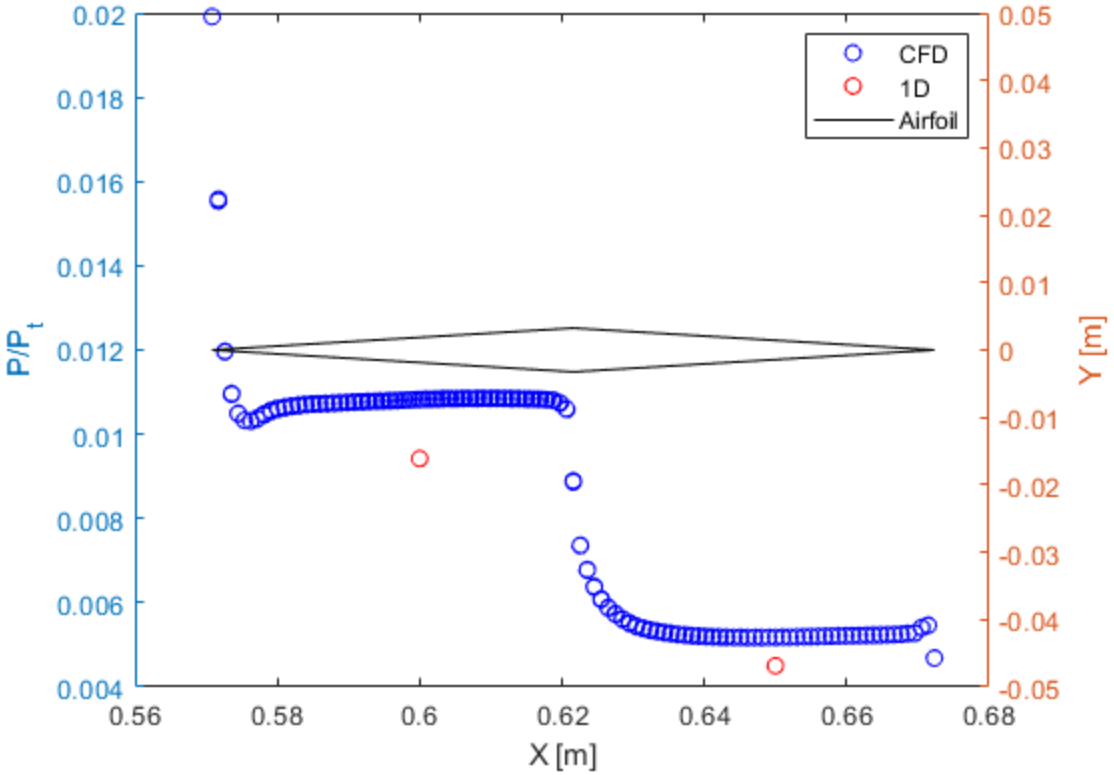

Note the behavior of the expansion fan over the turn from the front to rear face.

Figure 8 Airfoil static pressure along chord line in Mach 4 flow.

Isentropic flow parameters, oblique shocks, and Prandtl-Meyer flow relations predict a forward face, static-to-stagnation pressure ratio of 0.00942 and a rear face pressure ratio of 0.00450 based on the upstream conditions. Note that the pressure ratios indicated by the chart are slightly higher at 0.0108 and 0.00519 respectively due to losses in the boundary layer. The closeness of the results obtained from CFD to those derived analytically enhanced the confidence in this method and allowed for its application and confidence in testing the flows created by new geometries. Again, this development is central to progress in the project, as the flow conditions created by a given geometry can be validated before hardware for the construction of the tunnel is procured.

B. NOZZLE GEOMETRY GENERATION

Though the test section-to-throat area ratio can be calculated by the means of a simple equation, achieving a geometry that would connect those two dimensions while also expanding the flow as ideally as possible is much more involved. To address this issue, a numerical method of characteristics MATLAB code called "Supersonic Nozzle Design Tool" by Dodson was utilized [6]. Essentially, the code takes an input desired Mach number and a desired number of expansion waves with which to model the geometry. The expansion waves serve to adjust the resolution of the nozzle shape, which produces a uniform inviscid flow at the test section. This allowed a more accurately shaped fluid domain in later CFD studies and in the construction of a solid model for later production. The code then returns a dimensionless set of X and Y coordinates outlining the nozzle shape. This output is demonstrated visually in Figure 9. Though the throat-to-test section geometry was fully calculated by this code, the converging and diffusing sections of the nozzle (also important to the tunnel operation) were not.

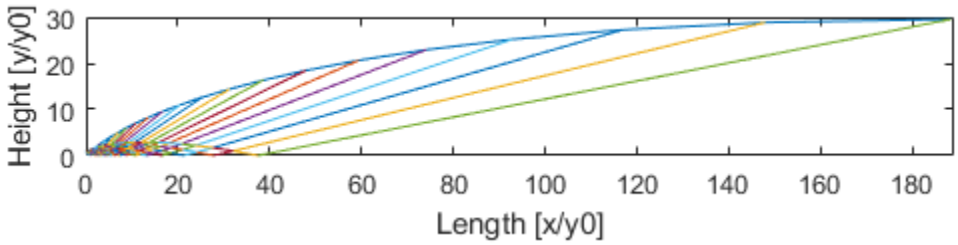

Figure 9 Method of characteristics nozzle geometry output.

Engineering drawings with the dimensions of the Mach 4.0 tunnel geometry were consulted both for CFD and for the converging and diffusing sections of that nozzle to be adapted to the new geometry. A MATLAB code titled "Design.m" was written to scale the converging and diffusing geometries as well as to scale the output of the supersonic nozzle tool, and to combine those two curves into a single array of points for exporting to a CAD modeler like Solidworks. Once imported to Solidworks, a smoothing spline was applied to the array of points and the geometry was enclosed and extruded to form a physical fluid

domain to be utilized for validation in computational fluid dynamics. The output of the geometry file from the MATLAB code is shown in its CAD presentation in Figure 10. It is important to note that these geometries are generated based on an assumption of an inviscid fluid, therefore ignoring the boundary layer growth that will shrink the effective nozzle area ratio and therefore decrease the test section Mach number.

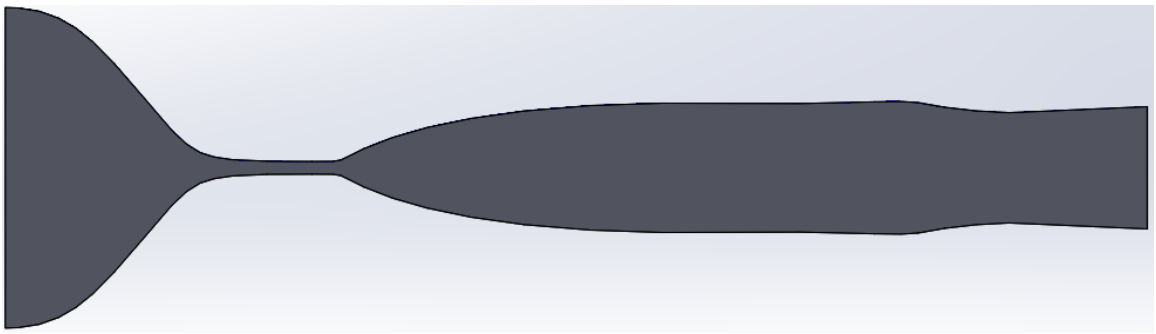

Figure 10 Mach 4 nozzle geometry generated by MATLAB code.

C. MACH 5+ NOZZLE DESIGN

At this point designs were produced attempting to form a reliable test section core flow at or above Mach 5.0. Note that the geometry production and CFD methods referenced in this chapter are identical to those described in Section A. This process took place relatively quickly, though the CFD mesh sizes required to resolve the flow fields in three dimensions quickly exceeded millions of nodes. However, most simulations could be performed within the span of 48 hours, which is relatively quickly compared to the time requirements of more complex simulations. Several different geometries were designed and modified, all with the goals of producing a stable Mach 5+ test section condition.

1. Modification to Half-Liner Geometry

The first three-dimensional simulation we performed was a fully symmetric Mach 4.0 nozzle. A full Navier-Stokes regime with Shear Stress Transport turbulence model was implemented. The results become troubling when observing the test section flow in the YZ plane. Looking at the test section from the perspective of the nozzle outlet, this cross

section shows a turbulent vortex forming on the sidewall at the mid-plane, or directly in the middle of the test section. This is troubling as test articles spanning the width of the test section will encounter this flow disturbance, producing results less comparable to those experienced in free-stream flow. This perspective can be observed in Figure 11. Figure 12 shows that this turbulent structure grows into the core flow as it continues down the length of the nozzle.

Because of the potential of this flow characteristic to disturb and skew future experimental results, options were evaluated to move the vortex out of the core flow field. It was hypothesized that by making the nozzle symmetric in XY with a flat wall along the XZ plane, the vortex would be evacuated to the upper corner of the nozzle and thus would avoid any test articles placed in the mid-plane of the test section. Consequently, to maintain the same geometric profile, test section size, and nozzle area ratio, the X and Y dimensions of the nozzle were doubled. The new "Half Nozzle" configuration results can be observed in subsection 2. Similar figures for a fully symmetric Mach 5.0 nozzle can be found in Appendix B.

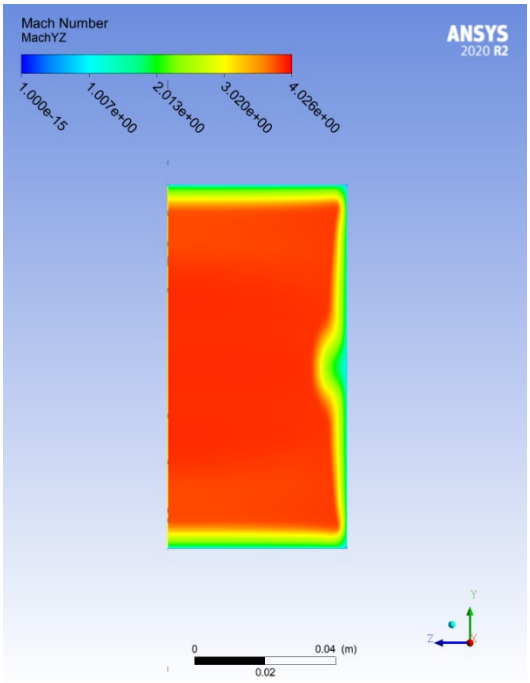

Note the growth of the semicircular structure on the side wall.

Figure 11 YZ plane Mach number distribution in Mach 4.0 test section.

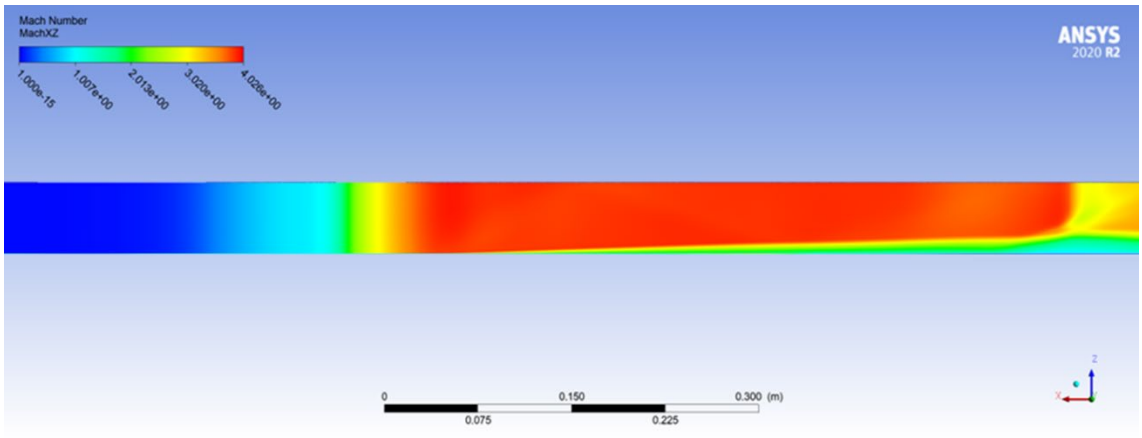

Note again the growth of this structure from the throat (right) to the outlet (left).

Figure 12 XZ plane Mach number distribution in Mach 4.0 nozzle.

2. Mach 5.2 Nozzle

Keeping in mind that the MATLAB code utilized in the nozzle curve generation did not account for the effects of viscous boundary layers, it was decided to design a nozzle to Mach 5.2. The initial hypothesis for the Mach 5.2 nozzle was that the higher goal Mach number would, after boundary layer-induced area ratio reduction, result in a core flow Mach number still greater than 5.0 and thus exceeding the design goal for the Mach 5+ wind tunnel. The results of this attempt can be observed in Figure 13 and Figure 14. The evacuation of the sidewall vortex to the top corner is confirmed by Figure 15.

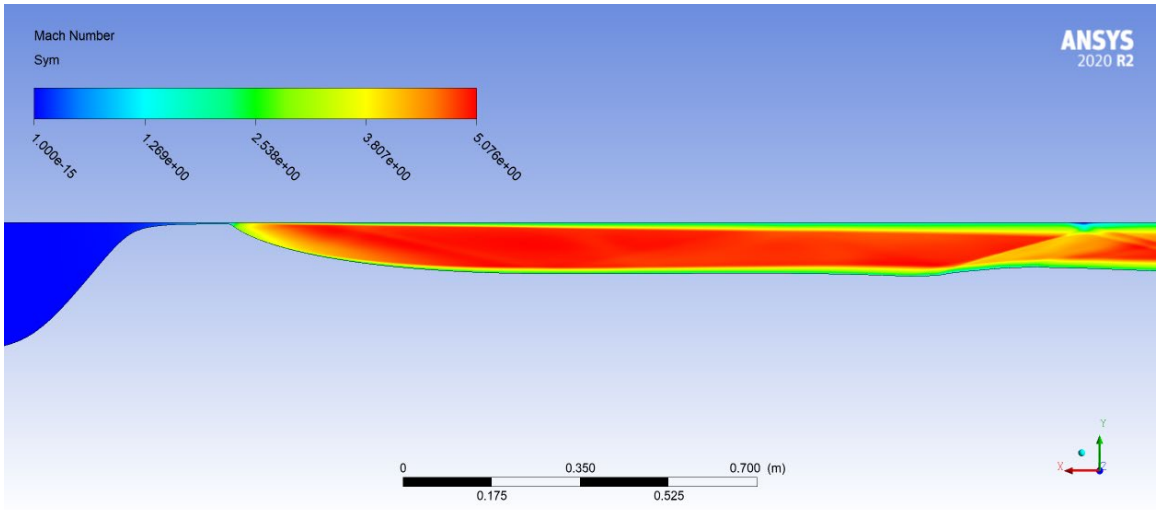

Figure 13 Mach number distribution for Mach 5.2 nozzle.

Figure 13 and Figure 14 make clear the effect of the boundary layer growth on the core flow Mach number. Though a Mach number above 5.0 is present in the initial, diverging portion of the nozzle, excessive boundary layer growth toward the outlet results in a contracting core flow area and a resulting lower Mach number. These results make it apparent that the growth of the nozzle in the X dimension as the desired Mach number increases counteracts the effect of the higher Mach number, still resulting in a test section Mach number below 5.0. Because this method of increasing the core flow Mach number is ineffective due to excessive boundary layer growth, the next step is to produce a boundary layer-modified geometry that expands to maintain the effective nozzle area ratio to produce a Mach 5+ flow.

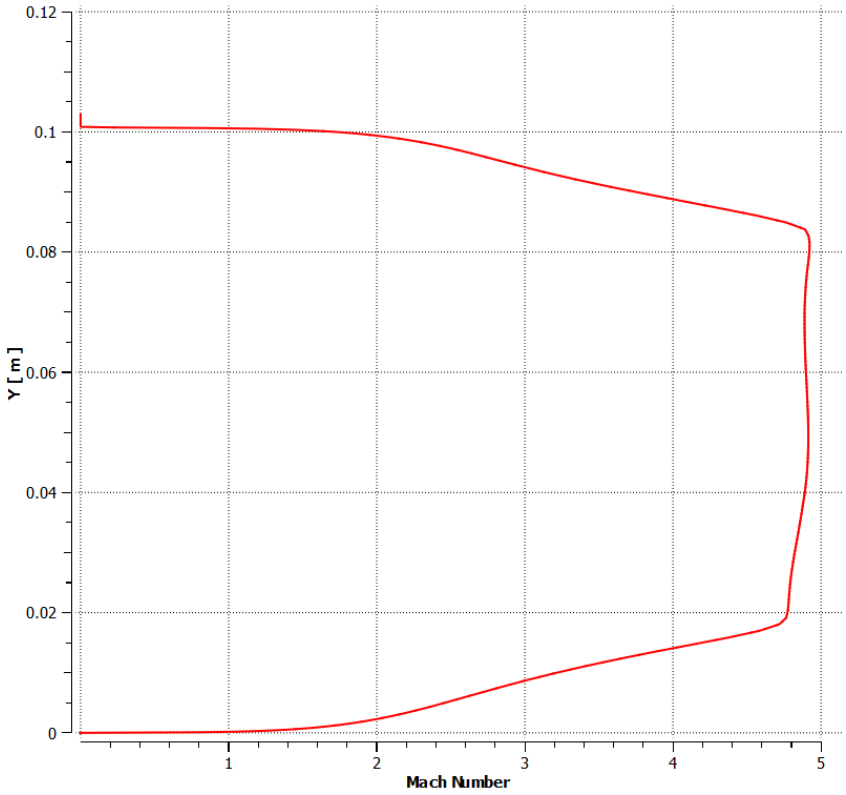

Note the thickness of the boundary layers in this case at nearly 2 centimeters.

Figure 14 Test section Mach number distribution for Mach 5.2 nozzle.

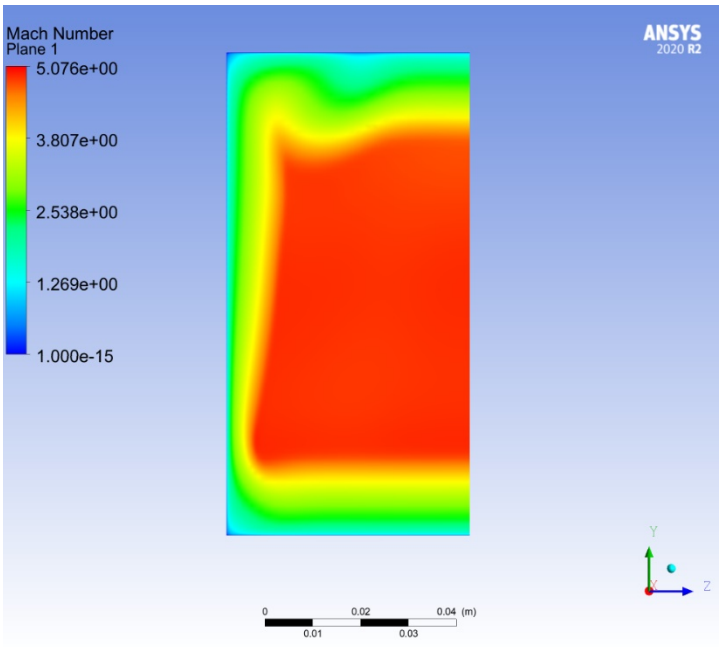

Figure 15 YZ plane Mach number distribution of Mach 5.2 "half-liner" nozzle.

3. Modified Mach 5.2 Nozzle

The production of the half-liner nozzle in the earlier case was performed by scaling the X and Y dimensions of the design code, as well as the current converging and diffusing geometries from the Mach 4 wind tunnel, by two. It took CFD analysis to observe the effect of the greatly elongated geometry on the growth of uncompensated boundary layers, thus decreasing the test section Mach number by decreasing the effective nozzle area ratio. Achieving the desired Mach number would require one of two modifications: offsetting the nozzle wall by the momentum thickness of the boundary layer or shortening the test section to constrain the boundary layer growth.

The calculation of the momentum and displacement thickness and shape factor is not inherently difficult. What is more complex is applying each of those expressions to the code-generated geometry precisely enough to overcome the viscous effects while still performing and ideal expansion of the flow field. Due to the complexity of data processing as well as the time requirements of this task, this approach was foregone in favor of the second one.

The current Mach 4 tunnel has a test section approximately 0.1143 meters long. Due to the scale of the Mach 5 geometry, the test section of the first version of the Mach 5.2 approached 0.9144 meters long. This was a result of an arbitrarily made design decision to scale the geometry of the wind tunnel globally as opposed to the diverging nozzle locally. This led to increasingly high Reynold's numbers in the test section and, as a result, extremely thick boundary layers. Because any experimental instrumentation would take up no more than the 0.1143 meters previously allocated in the supersonic wind tunnel, there is no need to scale the diffuser geometry beyond its current dimensions. Therefore, the nozzle becomes much shorter, the boundary layers much thinner, and the test section Mach number above the 5.0 target. This is shown clearly in Figure 16, Figure 17, and Figure 18.

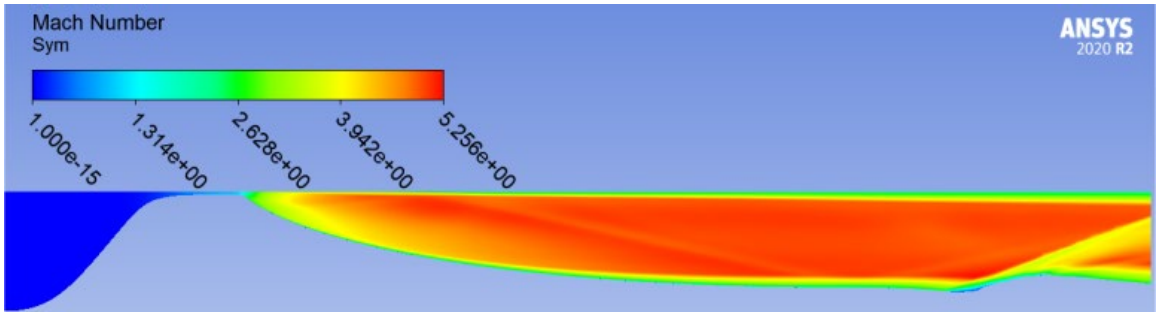

Figure 16 Symmetry plane Mach number distribution for final nozzle.

Figure 17 and Figure 18 show clearly that the design goals of uniform flow in the test section and core Mach number exceeding 5.0 are both satisfied. This final CFD gives us enough confidence to move on to the conceptual design stage and build a support structure that will allow the nozzle to operate reliably at the target Mach number. This process is discussed in detail in the following chapter.

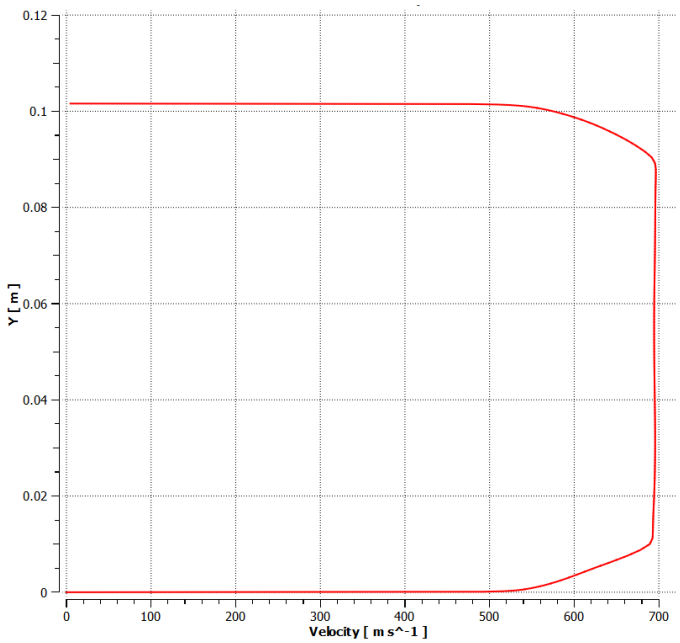

Figure 17 Test section velocity profile for final nozzle.

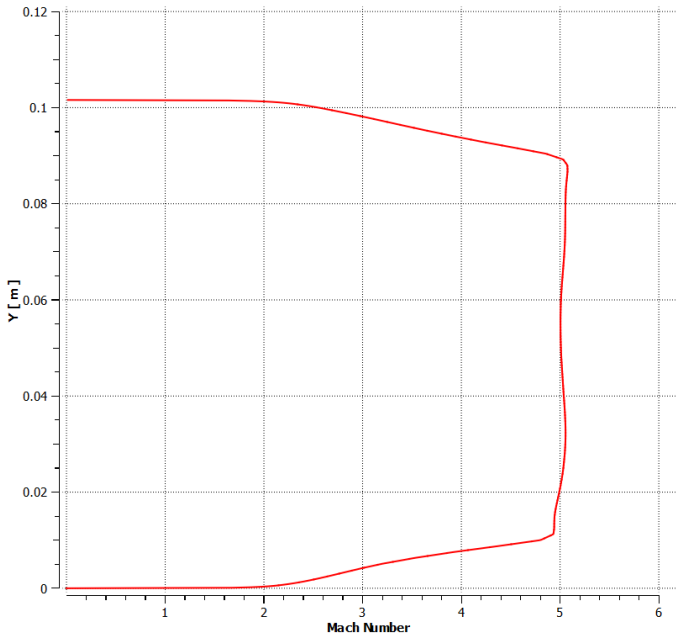

Figure 18 Test section Mach number profile for final nozzle.

IV. CONCEPTUAL DESIGN STUDIES

A. TUNNEL CONFIGURATION

The gas dynamics laboratory at the turbo propulsion lab has dimensions that would support two distinct tunnel configurations. Each configuration essentially changed the orientation of the optical axis in order to minimize distortion on fluid imaging experiments. The "high tunnel" configuration, depicted in Figure 19 involves extending the tunnel from the lead pipe and across the room on the same horizontal axis. The portholes of the test section in this case would be aligned vertically to accommodate an optical axis extending to the 30-foot ceiling. The primary benefit of this configuration is the elongated optical axis, minimizing the distortion in imaging processes. The primary drawbacks are the construction of a superstructure to hold all the components and an experimental platform, and the lack of vertical space with which to place critical components.

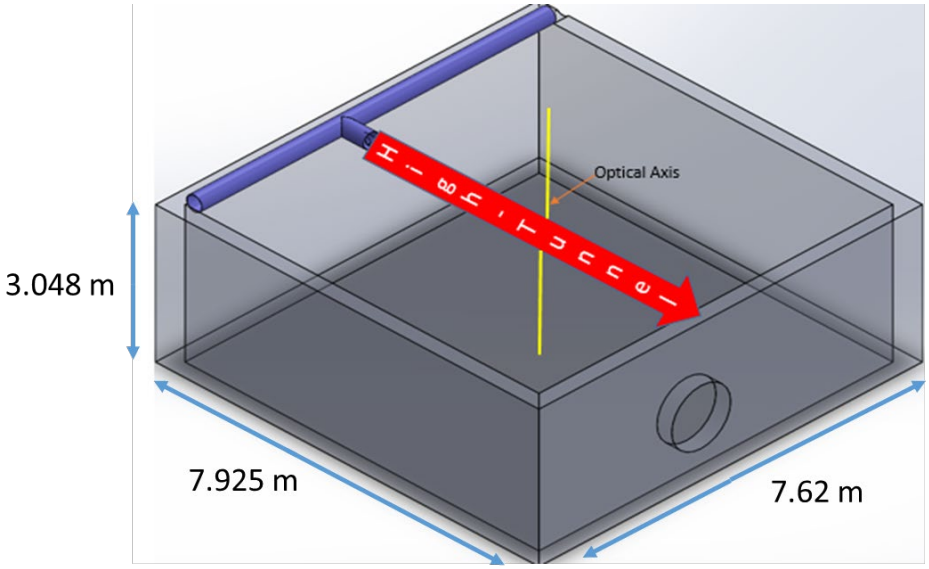

Figure 19 "High tunnel" configuration.

The "low-tunnel" configuration depicted in Figure 20 is the other option. This will place the test section closer to ground level, with two elbows descending the lead pipe

through a valve toward the ground before returning the flow axis to the horizontal axis. The portholes would be aligned horizontally to accommodate an optical axis extending across the base of the room horizontally. The primary benefit of this configuration is the lack of a superstructure requirement and the ease of experimentation interchangeability. The primary drawback is the shorter optical axis.

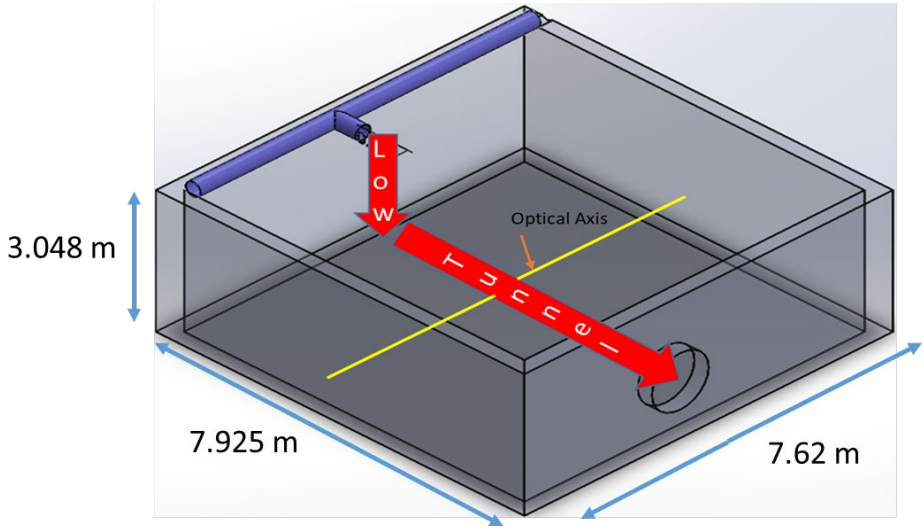

Figure 20 "Low tunnel" configuration.

Considering the benefits and drawbacks to design a tunnel most practical for regular operation resulted in the choice of the "low-tunnel" configuration. This tunnel would place the test section closer to the ground and thus not necessitate a support stand for the operators nor supplemental equipment to elevate the extremely heavy test section in place. The shorter optical axis would still be sufficiently long to ensure that any imaging data will have acceptable resolution. This tunnel will also allow additional space for surplus heating and flow straightening equipment. The decision on the general configuration of the tunnel now enables the progress into the design phase of the tunnel components and the test section.

B. TEST SECTION DESIGN

Test section design involved the incorporation of the nozzle design developed in Chapter III to fit and function properly with the rest of the tunnel hardware. Solidworks was used as the design tool during this process as it allowed the evaluation and verification of the dimensions and the incorporation of different components into a singular solid model. It also facilitated the realization of other facets of design not previously realized, such as the necessary creation of custom components to feed the air supply into the test section, the incorporation of the heat exchanger (discussed further in section C), and the method by which the flow will be exhausted back to atmosphere.

Accordingly, the design of the nozzle block itself was not as simple as extruding the designed curvature out of a solid piece of metal. The nozzle block design also had to account for the incorporation of sealing components, side and top boundaries, portholes, and instrumentation, all while providing enough fasteners to support its weight. The final form of the nozzle block and top wall is displayed in Figure 21.

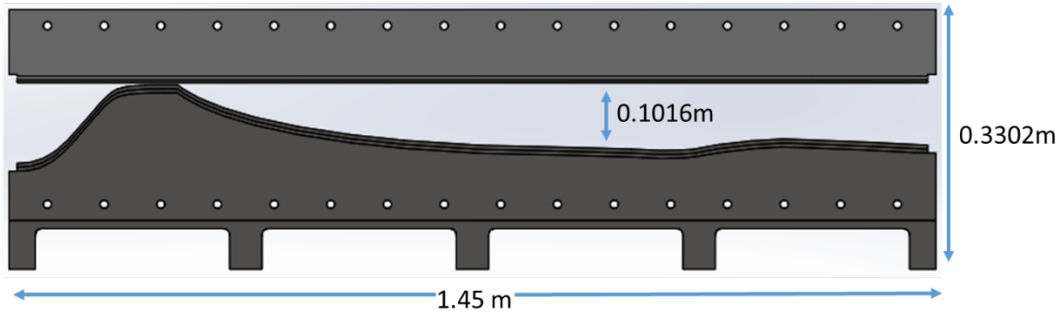

Figure 21 Nozzle block and top wall with primary dimensions.

The nozzle block (bottom portion of Figure 21) will require incredibly precise machining and polishing to ensure the fluid flows over a smooth surface to minimize the height of the boundary layer. The stagnation temperatures encountered by the surfaces in contact with the fluid will be in excess of 450K, thus requiring them to be machined from stainless steel. A nozzle block of these dimension, when machined from cast stainless steel,

will have a mass of approximately 153 kg. The top wall will likewise be machined from cast stainless steel and will have a mass of approximately 71 kg.

The sidewalls were designed to connect the top wall with the nozzle block, constrain and seal the flow field, incorporate portholes, and contain fastening holes for support brackets to hold the test section to the upstream and downstream components of the tunnel. The left and right walls are identical as the placement of all drilled and cut holes is symmetric. The sidewall geometry is depicted in Figure 22. Each sidewall will be machined from 1-inch stainless steel and weigh approximately 70 kg.

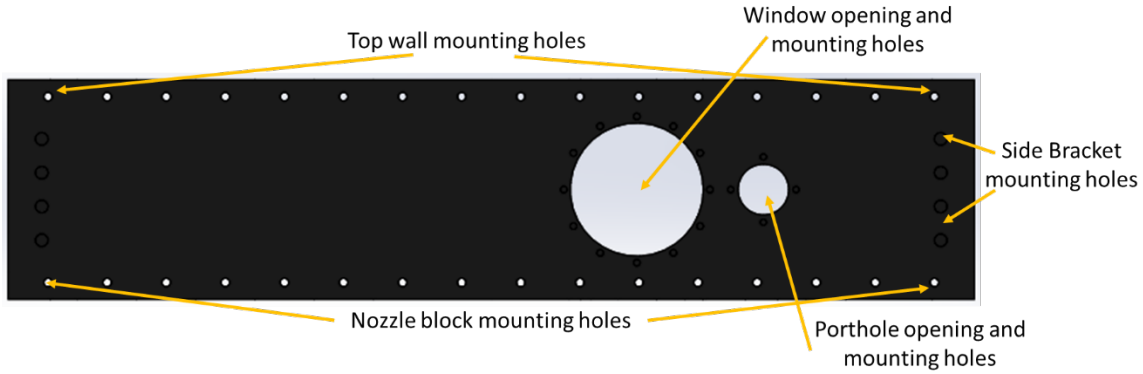

Figure 22 Annotated sidewall design.

The brackets were designed arbitrarily and with no real requirement but to support and align the test section with the upstream components. Their completion allowed for the assembly of the individual components into the complete test section, shown in exploded and assembled forms in Figure 23 and Figure 24 respectively. Note that the total mass of the test section and all included components is approximately 390 kg. Following the assembly of the test section, the next step in the design challenge was the incorporation of the heater, discussed in greater depth in section C.

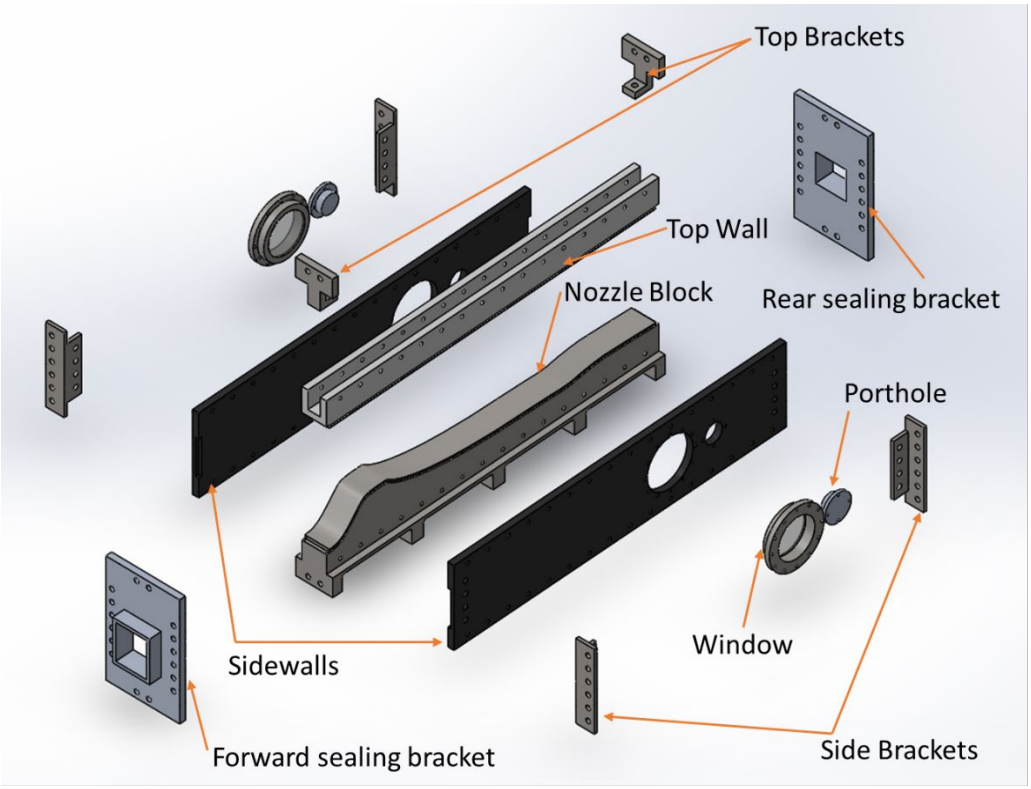

Figure 23 Exploded view of test section assembly.

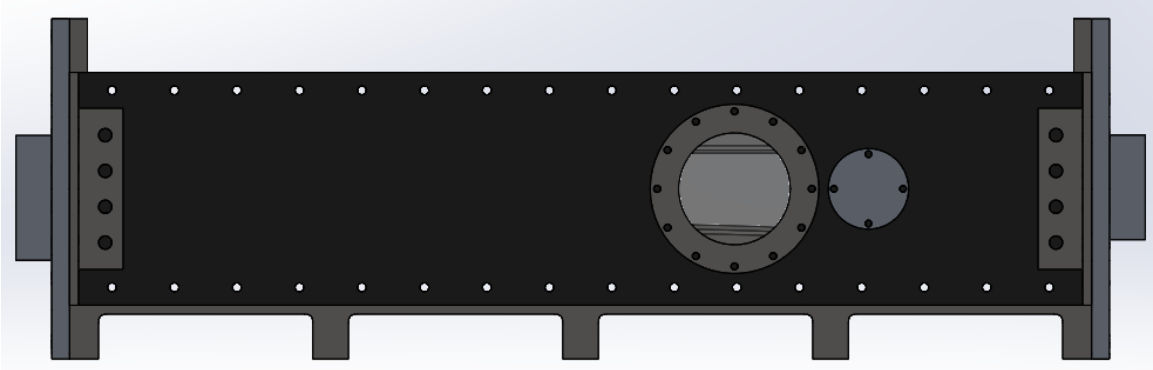

Figure 24 Assembled view of test section assembly.

C. HEATER SPECIFICATIONS

Chapter II section C details the method by which the necessary temperature increase to the upstream flow was determined. Combining this value with the specific heat of air at constant pressure (C_p) and the mass flow rate of the air produces the enthalpy rate,

or power required, of the potential heater. In the case of the test section already designed, this power requirement works out to approximately 200kW. To minimize the impact of the heating coils on the flow qualities on the outlet end of the heater, it was decided to search for a heater with the same interior diameter as the up and downstream piping as well as the greatest number of heating elements possible. This will prevent the formation of large jets causing unsteadiness and high free-stream turbulence on the outlet end. It will also minimize the total pressure drop experienced across the heating process.

To ensure the heater will not have to operate at its max rated heat load, it was decided that a heater capable of delivering 250kW would be adequate. Also necessary was ensuring whatever heater is ordered will operate in the 480V/400A electrical system currently in place in the lab. PID temperature control is also desired as being able to control the fluid temperature will be necessary for data accuracy and precision. One quote revealed a heater consistent with all of those requirements and delivering the metrics of performance demonstrated in Figure 25. A visual rendering of the heater in reference can be found in Figure 26.

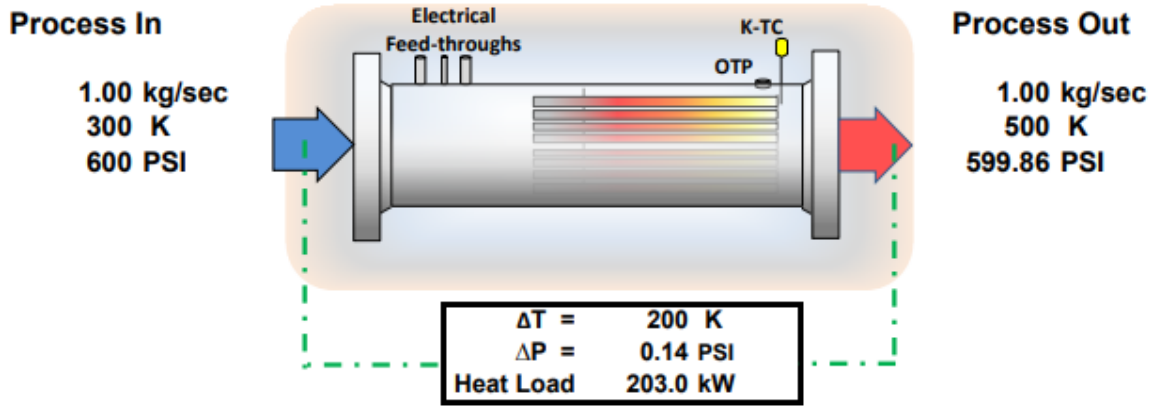

Figure 25 Heater performance diagram. Adapted from [7].

Figure 26 Visual rendering of TUTCO heater. Adapted from [8].

Though no information on the mass properties of the heater are available, the dimensions were given and a budget of $95,000 quoted. The next step was incorporating the heater into the tunnel model and completing the solid model of the entire system.

D. OVERALL TUNNEL DESIGN

The completion of the test section design and heater dimension allowed for the design process to carry into the final stage of constructing the global solid model of the complete system. Previously procured hardware was modeled and incorporated into the design to fit the "low tunnel" configuration previously chosen. The result of this construction can be observed in Figure 27 and Figure 28. Note the inclusion of the vertical support stands for supporting the weight of the tunnel and the singular horizontal support stand designed and placed to counteract the thrust and moment produced by the fluid flowing through the tunnel. Also note that the diffuser will exhaust to the atmosphere outside. The 6' humanoid object included in each figure is intended to give the reader an idea of the tunnel size and the size of the room that houses it.

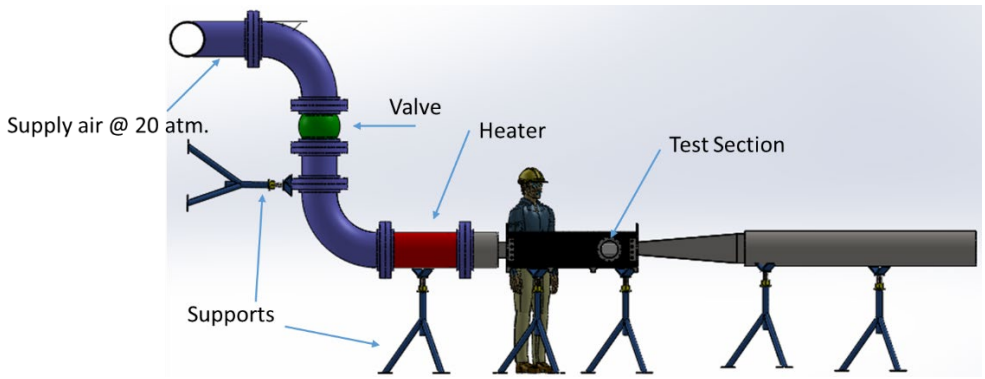

Figure 27 Side view of tunnel assembly.

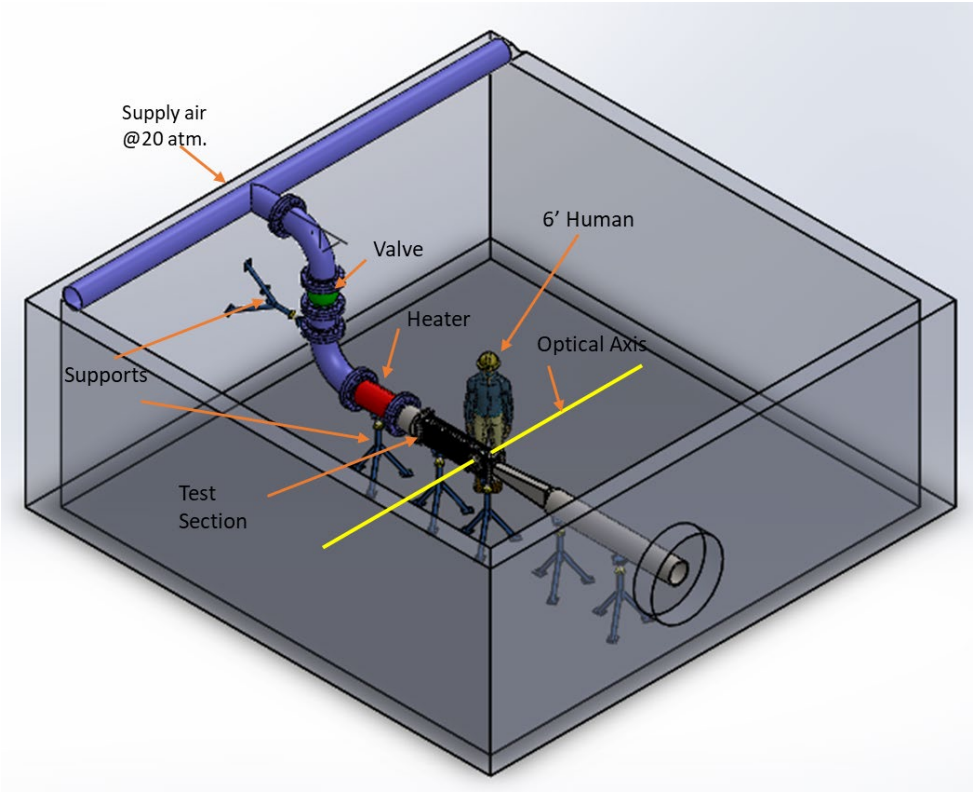

Figure 28 Isometric view of tunnel assembly.

This model is mostly complete but leaves room for the adoption of the sting balance and the particle image velocimetry systems. The summary of what has been completed and what remains will be discussed further in chapter V.

V. CONCLUSION

A. STATUS OF THE PROJECT

The goal of this project at the outset was to lay the foundation for the modification of the current supersonic wind tunnel at NPS to one capable of accommodating hypersonic flows. Many steps were completed in pursuit of that goal. CFD analysis of the current supersonic wind tunnel geometry, not yet performed to this point, has been completed in great deal and also revealed a novel topic in supersonic wind tunnel design in the discovery of the midline vortices. This is a topic most recently published upon by researchers at Cambridge and the Air Force Research Laboratory in the AIAA Journal in March 2021 [9]. This connection certainly demonstrates an advantage of exploratory research and lays the groundwork for the use of CFD as a wind tunnel design tool.

The validation of a CFD method with which to analyze wind tunnel design allowed for the adaption of an inviscid (method of characteristics-based) design to a fully validated, viscous Mach 5+ tunnel. The flow qualities were then analyzed to determine other outstanding requirements for the tunnel's construction (i.e., the heater) and the construction of the test section. Finally, previously procured and newly designed hardware was modeled computationally to assess the effectiveness of new design features to be incorporated in the NPS Gas Dynamics Laboratory in pursuit of an experimental flow field exceeding Mach 5.0.

B. FUTURE WORK

Recommend that future work adapt and refine the previously completed design for ease and affordability of manufacturing as well as ease of integration and one-person operation. The solid models and designs constructed and evaluated in this project may serve as a steppingstone to procuring the necessary hardware, and assembling and testing it. The desired end state is a high-runtime, Mach 5+ flow field that will undoubtedly enhance the reputation of NPS as a premier aerospace research and learning facility.

THIS PAGE INTENTIONALLY LEFT BLANK

APPENDIX A. CFD METHOD SUPPLEMENT

Employing the Method of Characteristics in Supersonic Nozzle Design

ENS Connor J. Aspray

ME4225 Term Project

Introduction

This study accompanied research in pursuit of the design and construction of a Mach 5 supersonic wind tunnel at NPS. The intent was to utilize the method of characteristics to produce the geometry for an ideally expanded Mach 5 nozzle and to validate the effectiveness of this method with a full Navier-Stokes simulation in ANSYS CFX 19.2. The following report details the steps taken during the time period from August to December 2020 in pursuit of this objective.

Development of Validation Method

The majority of the time spent on this project was in pursuit of the development of a robust method through which a computational simulation could be implemented on a given converging-diverging nozzle geometry. Having knowledge of the flow field characteristics of the current configuration of the Supersonic Wind Tunnel (SSWT), the first attempted simulation was applied to the nozzle geometry designed to produce a Mach 4 flow field.

All simulations performed in this development imposed the total energy problem throughout the fluid domain. The initial geometry tested was a 2-D rendering of the Mach 4 nozzle, with a sweep method being applied to impose only 1 division across the 0.1 inch wide [z] domain. The settings were also adjusted to perform an inviscid simulation, setting the fluid viscosity to zero and each of the walls to a free-slip condition. The boundary conditions applied to the initial nozzle geometry were a subsonic, total pressure inlet of 12 atm. and a subsonic, static pressure outlet of 1 atm. reference pressure. Over the course of a thousand-or-so iterations, the residuals in mass and momentum converged to 1.0e-5. The imagery produced by the results indicated that the computational method was prematurely imposing normal shock in attempting to satisfy the subsonic outlet condition, though the rest of the flow field appeared to be accurate to the design, producing a test-section Mach number of approximately 4.04. The solution in reference can be found in figure 1.

To remedy the issue of the premature normal shock, a far-field boundary was imposed to attempt to capture both the location of the normal shock as well as the pressure ratio required to establish and maintain the flow field in the tunnel. The solution

in this stage remained governed by the Euler equations. Attempts to establish and capture the normal shock in the flow field were met with considerable hardship, due mostly to the instabilities of a flow field with no fluid viscosity. Attempts to employ a turbulence model in pursuit of greater fluid damping were unsuccessful. The visual of the flow field being referenced can be found in figure 2.

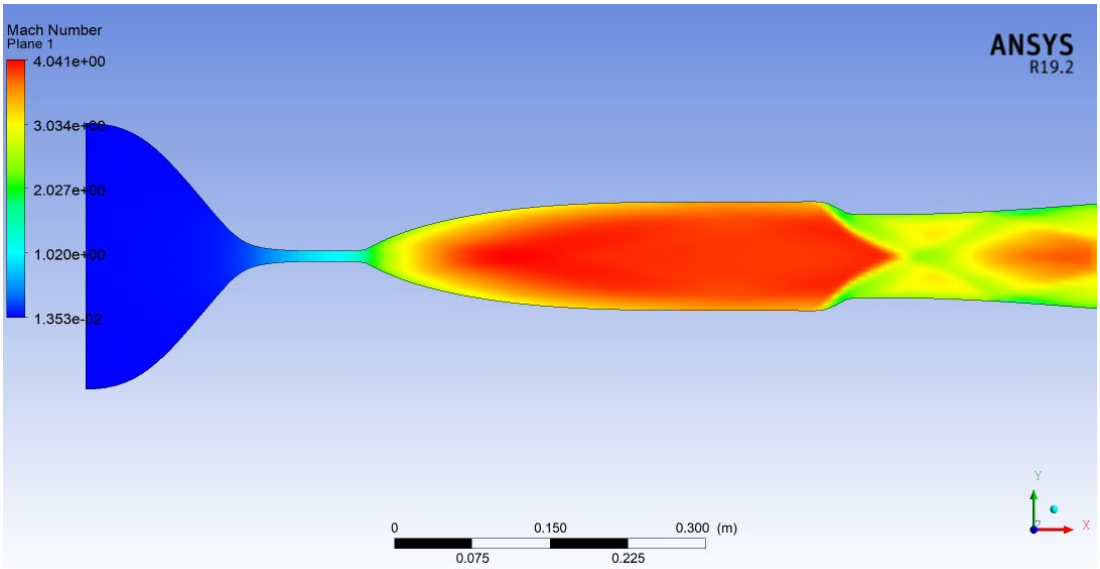

Figure 1. Initial Mach 4 flow field simulation.

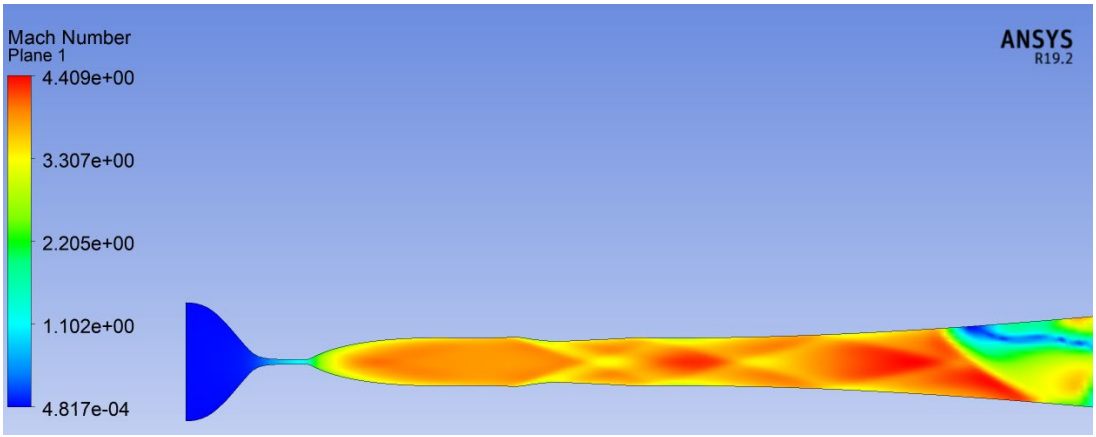

Figure 2. Far-field Mach 4 simulation with oscillating normal shock.

Though attempts were made at converging on a solution to the normal shock problem, the computations were consistently met with fatal overflow errors as the solution diverged over time. This is when Professor Hobson and I decided the boundary conditions may be the issue. In an attempt to model the realistic physical process of starting the tunnel, we decided to increase the inlet pressure gradually to computationally mimic the opening of the valve from the high pressure reservoirs to the tunnel. Keep in mind that the inlet condition is still based on the input total pressure. Though this gradual pressure rise did make the simulation more stable, convergence to the required 1e-5 RMS

residual was still unseen. To simplify the problem further, the fluid domain was shortened to a length that would be adequate to assume a supersonic outlet condition. However, there were still inherent instabilities that were due to the total pressure inlet condition. Therefore, the inlet was changed from total pressure to a mixed combination of static pressure and normal velocity. An arbitrary velocity of 10 meters per second was selected to accompany a gradually increasing pressure from 2 to 12 atmospheres. Because the contraction ratio of the nozzle was so large and the inlet Mach number so small, the static and total pressures were approximately equal though the static pressure condition finally stabilized the solution enough to converge.

To decrease the required human interface in the simulation, an expression was written to specify the inlet condition to increase from 2 to 12 atmospheres static pressure over the course of 1000 iterations. This 1 atm./1000 time steps appeared to be an adequately stable rate at which to increase the pressure.

Finally, because the solver would not accept a supersonic outlet as an initial condition, the initial outlet condition was a subsonic, average static pressure of 1 atm. for the first 1000 timesteps, followed by a change to a constant static pressure inlet of 12 atm. and a supersonic outlet. Finally, a solution was reached and the mesh further refined to obtain better resolution and more precise results.

To summarize, the method finally developed consisted of the following steps.

1. Employ an expression-based inlet condition to increase the static pressure at the rate 1 atm./100 iterations to the target inlet pressure. Impose an inlet velocity of 10 meters per second. Set a subsonic, average static pressure outlet of 1 atm.
2. Once the target inlet pressure is reached, set the inlet to the target static pressure and a velocity of 10 meters per second while changing the outlet condition to supersonic.
3. Allow the solution to converge on the coarse mesh (about 3% final mesh size) and then gradually refine the mesh to achieve greater resolution.

Now that a robust method was developed with which C-D nozzles could be consistently evaluated in the computational domain, the job shifted to creating the nozzle geometry required to expand the gas to the target Mach number of the SSWT of 5.0.

Method of Characteristics and Geometry Development

To both simplify the project and allow for greater CFD simulation time, the process of creating my own method of characteristics code for nozzle design was foregone and substituted with one of the many freely available codes on the internet. The code used in this project “Dozzle.m” is freely available on the MathWorks website under the title “Supersonic Nozzle Design Tool” and was authored by Cory Dodson.

The function took inputs of gamma, desired Mach number, and number of expansion waves (nozzle resolution) desired. It then created a dimensionless set of coordinates starting at the throat exit and ending at the nozzle exit scalable by y0, or the desired throat height of the nozzle. Since the exit height was desired in this scenario (to satisfy test section dimensions) the nozzle was instead scaled by the exit area. The non-dimensional output of the code is depicted in figure 3.

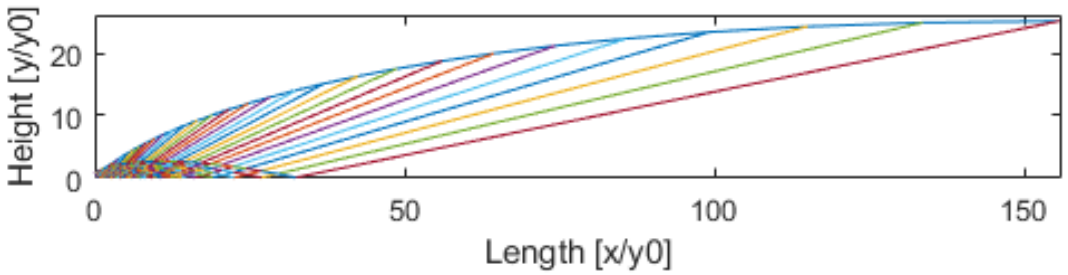

Figure 3. Non-dimensional geometry output by Dozzle.m

Since geometry was only generated from the throat exit to the nozzle exit, the existing inlet and diffuser geometry of the SSWT was scaled appropriately and applied to the model to create the computational domain.

Mach 5 Results and Validation

Using the method developed and the geometry from the MATLAB code, the first simulation would be a 2-D, inviscid validation of the test section Mach number desired in the SSWT. Over the first 1300 iterations, the inlet static pressure was gradually increased from 2 to 15 atm. while the inlet velocity was held constant at 10 meters per second and the outlet was held at a constant static pressure of 1 atm. After iteration 1300, the inlet static pressure was fixed at 15 atm. and the outlet was set to supersonic and the solution converged. After two refinements, the results were satisfactory to the desired specifications and the validation moved forward to a full 3-D, Navier-Stokes model. The 2-D simulation took less than one hour to complete and the results can be seen in figures 4, 5, and 6. The test section Mach number was less than 1% greater than the target of Mach 5.0, validating the ability of the geometry to form the desired flow field.

The original method of performing the full 3-D, Navier-Stoked simulation was to simulate one quadrant of the nozzle with symmetry planes on the interior XY and XZ planes. Though no issues were encountered in converging on a solution, the results looked peculiar in that a wake was growing from the throat to the exit plane on the sidewall. To determine whether or not this effect was likely real, the geometry was

transformed to a fully symmetric nozzle with a symmetry plane on the interior XY plane. This meant that half of the total nozzle was being simulated.

The viscous methods in each of these fully 3-D simulations were using the Shear Stress Transport model with no transition, the default dynamic viscosity of ideal air, and an inlet turbulence intensity of 5%. An artificial inflation layer was generated to capture the sidewall boundary layer using a biased sweep method with 100 divisions. The final mesh size was approximately 33,000,000 nodes and the total computational time was 24 hours and 50 minutes for the symmetric 3-D model.

Much to our chagrin, the vortex did not disappear in the fully symmetric geometry, leading us to believe that it is, in fact, a real effect. The results of this

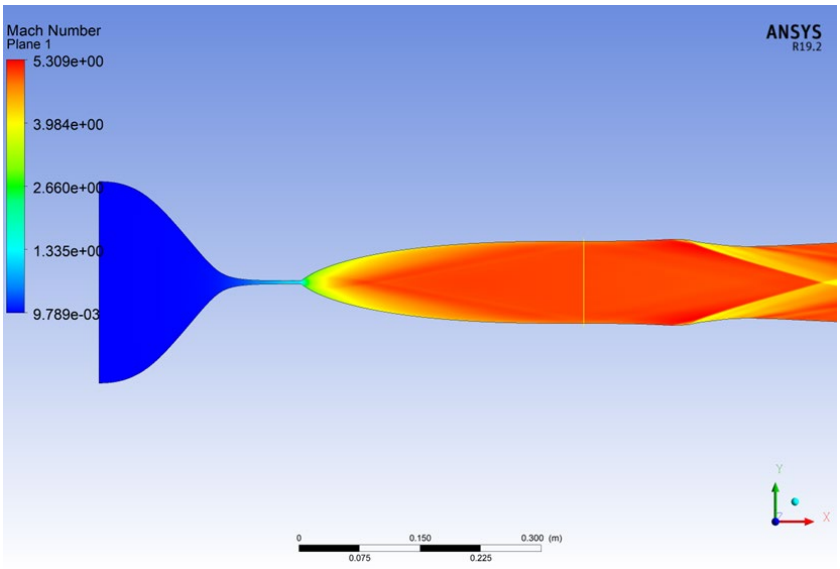

Figure 4. 2-D inviscid Mach number distribution in XY plane.

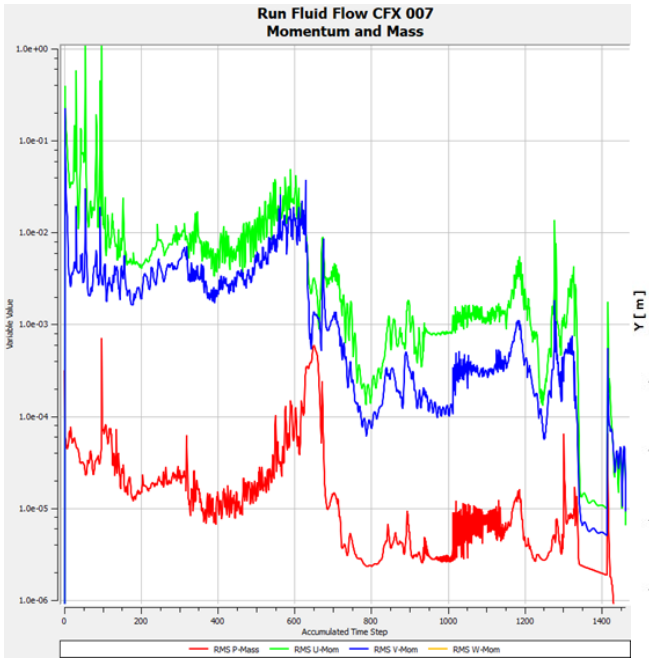

Figure 5. RMS residuals of 2-D, Mach 5 simulation.

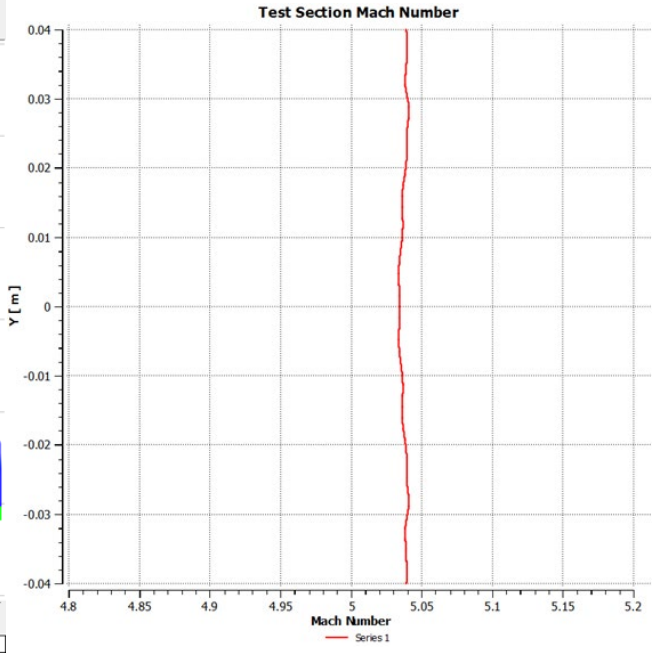

Figure 6. Test section Mach number distribution in Y for the 2-D case.

symmetric 3-D test case as well as the vortex can be seen in figures 7-10. The test section Mach number achieved in the symmetric 3-D case was approximately 4.9.

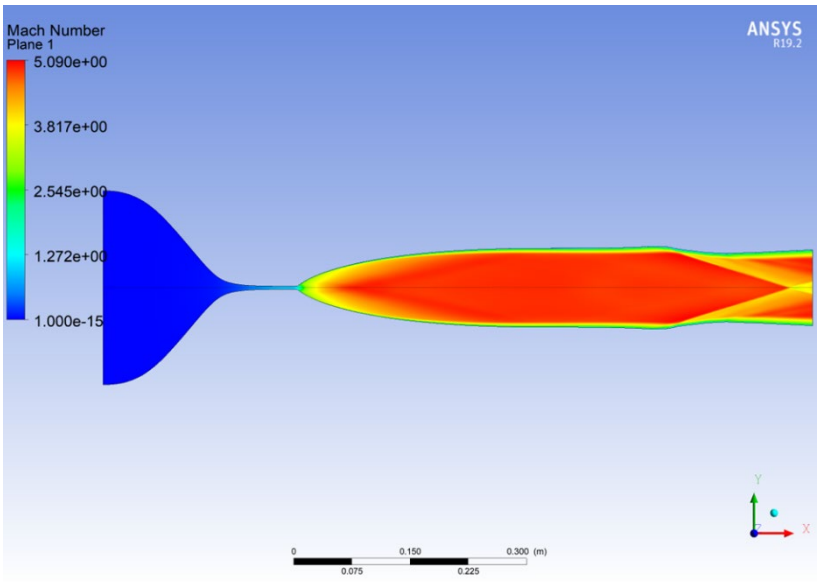

Figure 7. Mach number distribution in XY plane of symmetric 3-D case.

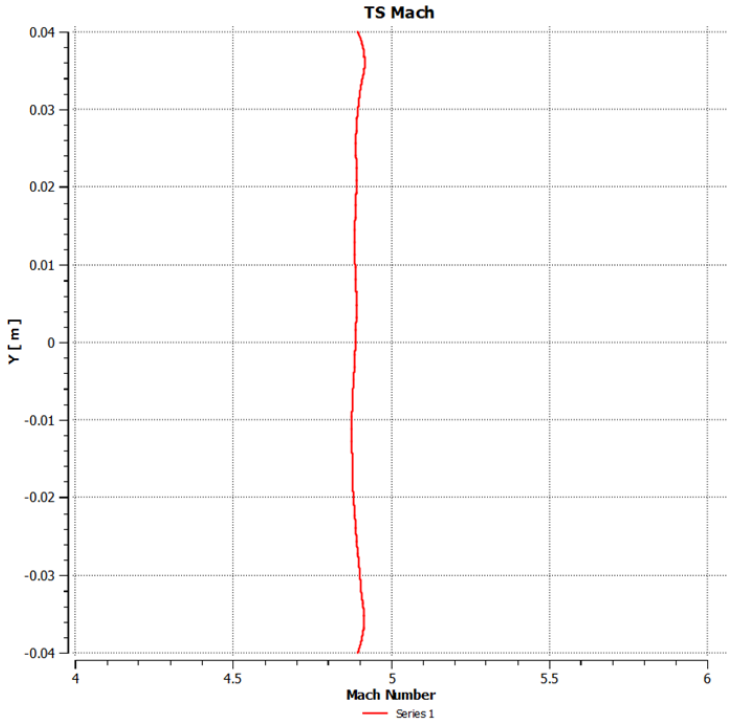

Figure 8. Test section Mach number distribution of 3-D symmetric case.

Because we were concerned of the potential of the vortex to interfere with any test articles due to its proximity to the test section, we modified the geometry to achieve the same test section size with a flat wall in the XZ plane. This moved the vortex to the bottom right corner of the tunnel. I refer to this case as the half 3-D model. The half 3-D simulation was performed with the same steps as detailed in the preceding paragraphs.

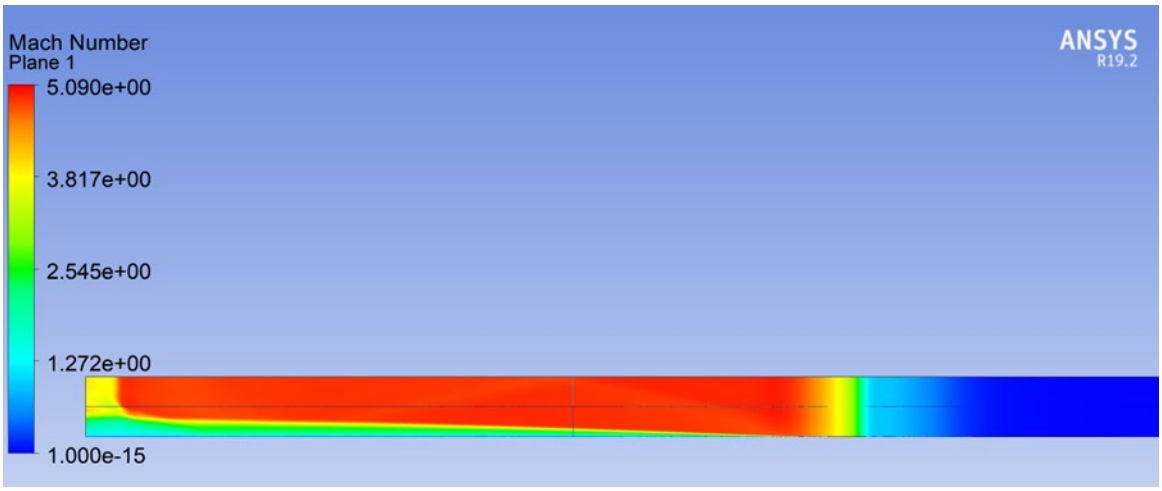

Figure 9. Inlet (right) to outlet (left) growth of vortex structure in XZ plane for symmetric 3-D case.

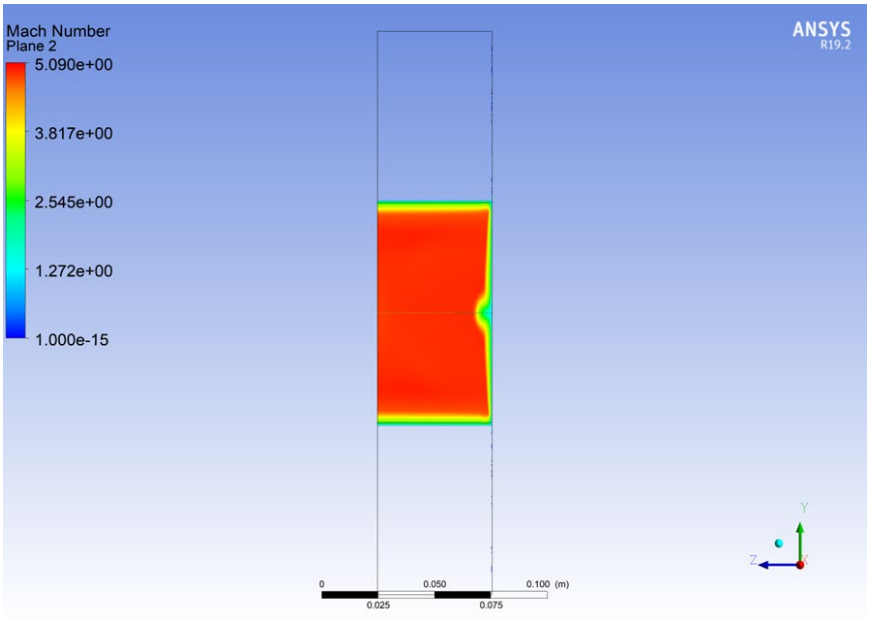

Figure 10. YZ plane of test section Mach number distribution of symmetric 3-D case.

The final mesh size was also approximately 33,000,000 nodes and the total compute time just short of 40 hours.

The test section Mach number for the half 3-D case mirrored that of the symmetric case almost exactly, sitting right around 4.9. Within 0.1 of the target of Mach 5.0 was deemed an acceptable deviation, validating the method of characteristics used for the creation of the Mach 5 nozzle. Results for the half 3-D case can be seen in figures 11-13.

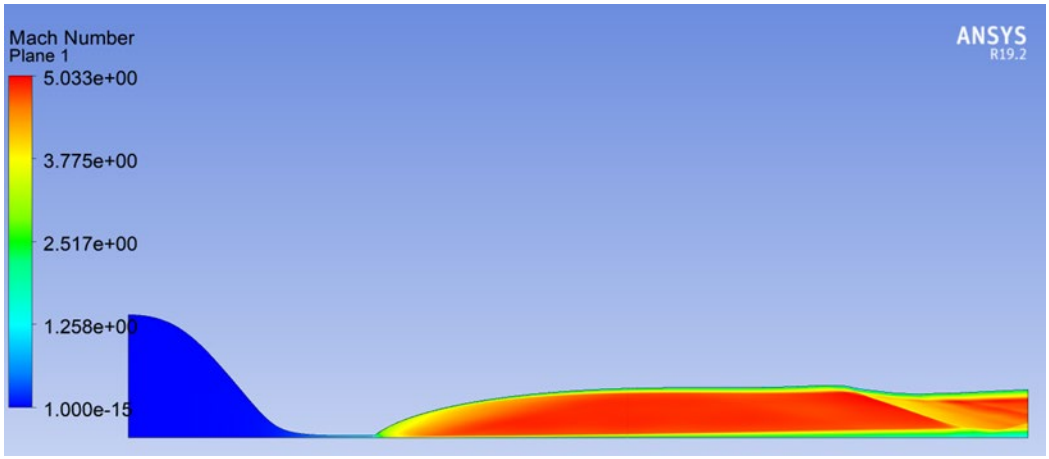

Figure 11. XY plane Mach number distribution of half 3-D case.

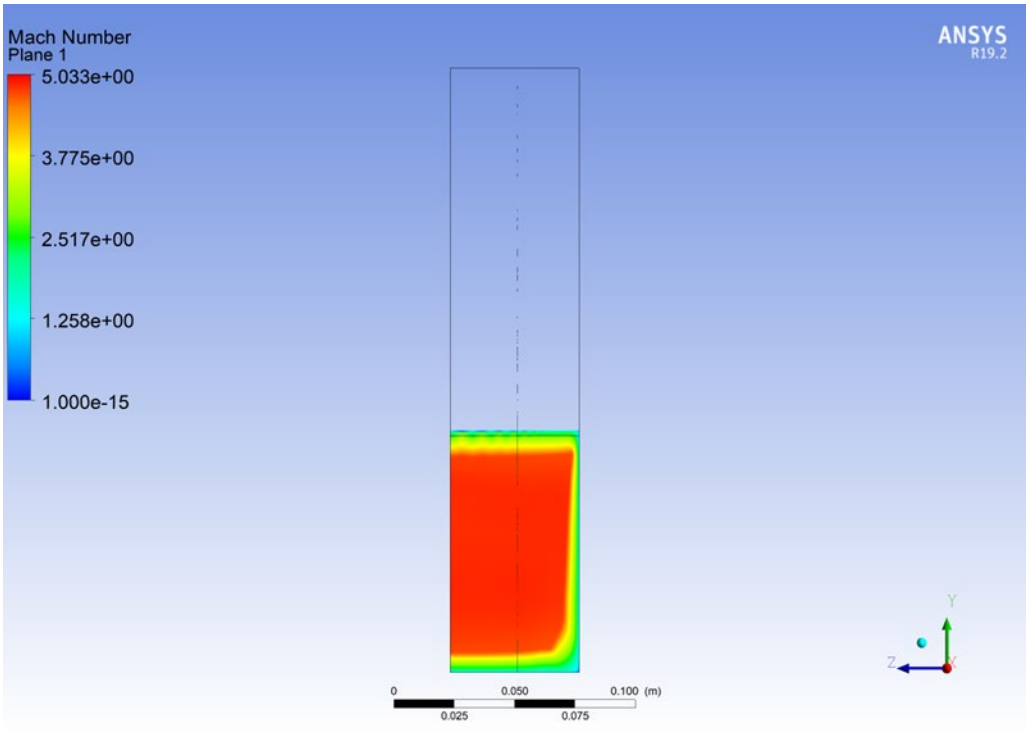

Figure 12. YZ plane view of test section Mach number distribution for half 3-D case.

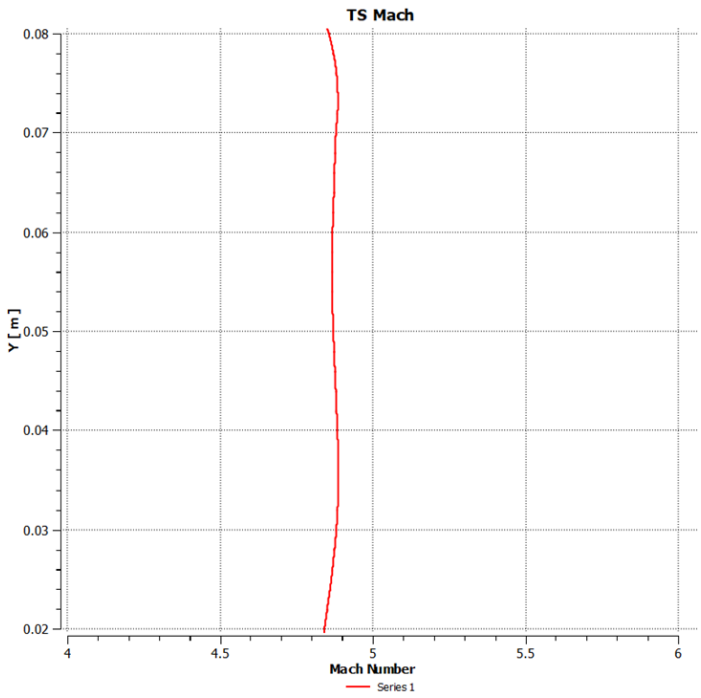

Figure 13. Test section Mach number distribution for half 3-D case.

Future Work and Application

Validation of the nozzle design through the simulations discussed above enables the investment required to machine these nozzle blocks to further validate their design in the real tunnel. Furthermore, additional computational research can be performed to better understand the design parameters of the SSWT and how changing the test section size will affect them. Further attempts at capturing the terminating normal shock will be made to achieve better predictions of mass flow and pressure ratios required to start and run the tunnel. The nature of the mystery wake emanating from the nozzle throat will also be explored.

Finally, a guide will be created to explain to other students how best to approach the problem of highly compressible flows in C-D nozzles and how to model them according to their real characteristics.

I would also like to thank Professors Hobson, Gannon, and Smith for their help and time in the pursuit of this project.

APPENDIX B. SUPPLEMENTAL CFD FIGURES

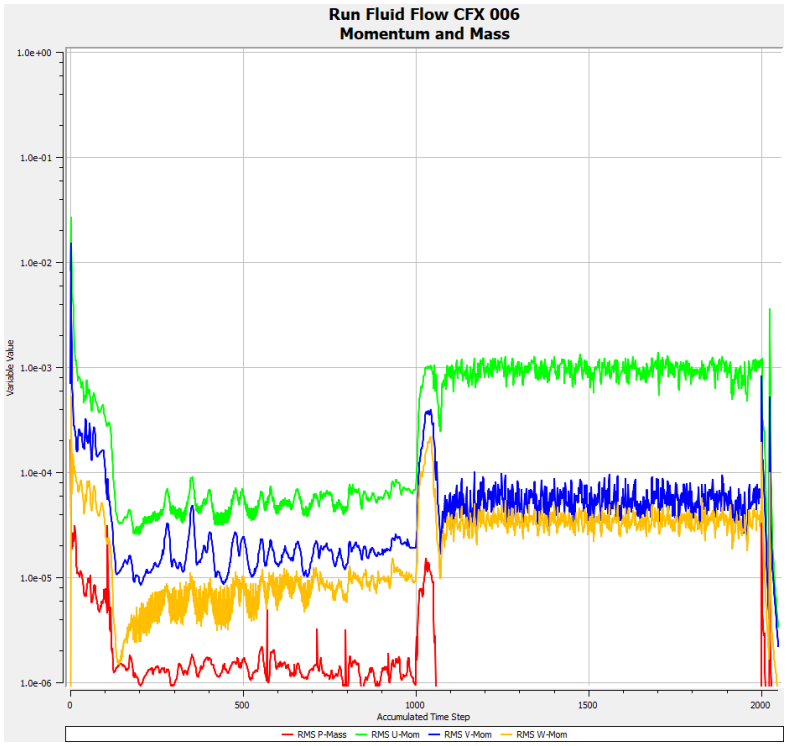

Figure 29 Fully turbulent, viscous Mach 4 residual convergence plot.

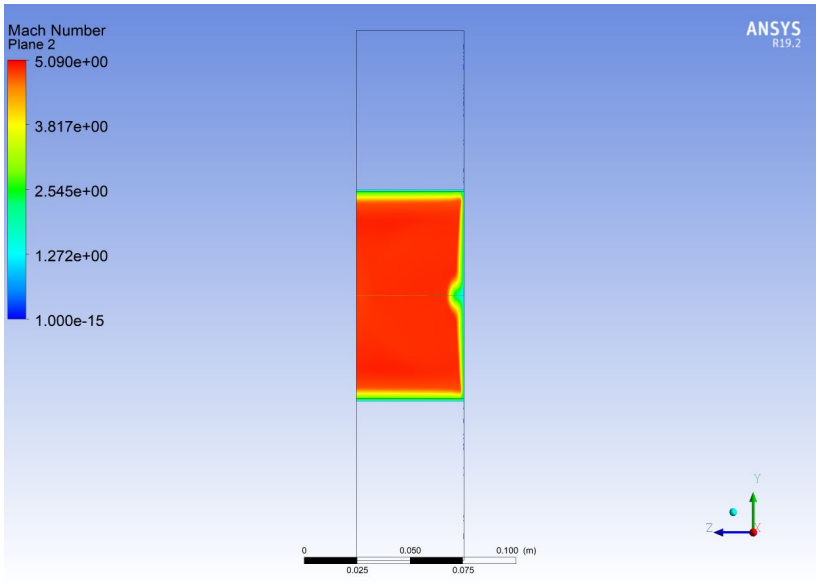

Figure 30 XY plane Mach number distribution in Mach 5.0 test section.

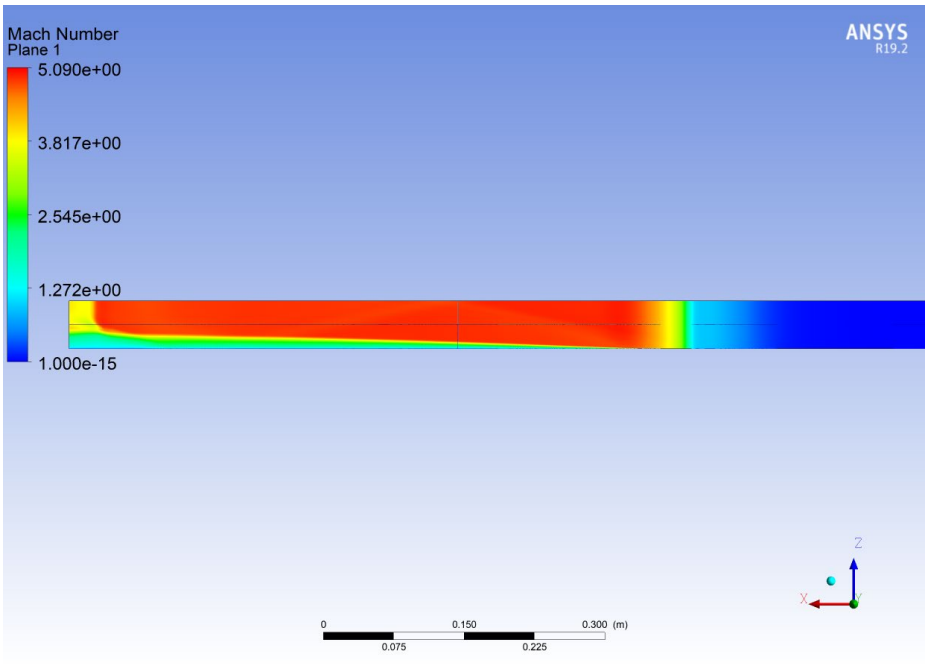

Figure 31 XZ plane Mach number distribution for Mach 5.0 nozzle.

LIST OF REFERENCES

[1] Mattis, J, 2018, "Summary of the 2018 National Defense Strategy of The United States of America: Sharpening the American Military's Competitive Edge,"

[2] Anton, P.S., Gritton, E.C., Mesic, R., Steinberg, P., et. al., 2004, "Wind Tunnel and Propulsion Test Facilities: An Assessment of NASA's Capabilities to Serve National Needs," RAND National Defense Research Institute.

[3] Naval Postgraduate School, 2021, "NPS Mission," from nps.edu/mission.

[4] Hobson, G., Gannon, A., and Smith, W., 2021, Turbo Propulsion Lab Faculty, Naval Postgraduate School, private communication.

[5] National Institute of Standards and Technology, 2021, "Thermophysical Properties of Fluid Systems." From https://webbook.nist.gov/chemistry/fluid/

[6] Dodson, C., 2021, "Supersonic Nozzle Design Tool," MATLAB Central File Exchange, from https://www.mathworks.com/matlabcentral/fileexchange/43212-supersonic-nozzle-design-tool?s_tid=srchtitle

[7] Drohan, D., 2021, Business Development Manager, TUTCO Sureheat, private communication.

[8] TUTCO Sureheat, 2021, "Custom Specialty Heaters." From https://www.tutcosureheat.com/site/pages/custom-specialty-heaters

[9] Sabnis, K., Babinsky, H., Galbraith, D.S., and Benek, J.A., 2021, "Nozzle Geometry-Induced Vortices in Supersonic Wind Tunnels," AIAA Journal, **59**(3), pp 1087–1098.

THIS PAGE INTENTIONALLY LEFT BLANK

INITIAL DISTRIBUTION LIST

1. Defense Technical Information Center
   Ft. Belvoir, Virginia

2. Dudley Knox Library
   Naval Postgraduate School
   Monterey, California